

# UVM ScholarWorks

## Studies On The Molecular Mechanism Of S-Tide Mediated Activation Of Pkg-Ia

Item Type	thesis;article
Authors	Charles, Joseph William
Download date	2026-05-09 14:30:43
Link to Item	<a href="https://hdl.handle.net/20.500.14849/2936">https://hdl.handle.net/20.500.14849/2936</a>

STUDIES ON THE MOLECULAR MECHANISM OF S-TIDE MEDIATED ACTIVATION OF  
PKG-I $\alpha$

A Thesis Presented  
by  
Joseph William Charles  
to  
The Faculty of the Graduate college  
of  
The University of Vermont

In Partial Fulfillment of the Requirements  
for the Degree of Masters of Science  
Specializing in Pharmacology

January, 2019

Defense Date: October 24, 2018  
Thesis Examination Committee:

Wolfgang Dostmann, Ph.D., Advisor  
Kalev Freeman, MD., Ph.D., Chairperson  
George Wellman, Ph.D.  
Anthony Morielli, Ph.D.  
Cynthia J. Forehand, Ph.D., Dean of the Graduate College

## ABSTRACT

cGMP-dependent protein kinases (PKG) are key players in intracellular second messenger signaling within many cellular systems throughout the body. Most notably PKG is known for its role in smooth muscle relaxation (Pfeiffer et.al, 1999). The I $\alpha$  PKG isozyme has been identified as the primary effector of the nitric oxide pathway (and serves to be a novel drug target). To date the overall knowledge of structure and function of PKG is lacking in terms of the mechanisms of activation and the structural orientations that coordinate them. Recently, our laboratory has solved the crystal structure of the regulatory domain of PKG I $\alpha$ , which revealed a previously unknown  $\alpha$ -helical domain dubbed the Switch Helix (SW) (Osborne et.al, 2011). The SW domain was found to be a site of interprotomer communication via hydrophobic interactions between its C-terminus and hydrophobic residues, named the nest located on the opposing protomer. Synthetic peptides derived from the SW domain, named S-tides, dose-dependently activate PKG I $\alpha$  (Moon et.al, 2015). In addition, the amino acid residues of the nest are in proximity to the cGMP binding site B. It was hypothesized that the binding site for S-tides (nest) and the cGMP binding site B interact and are co-dependent of one another.

The hypothesis of this thesis is the binding site for the S-tides (nest) and the cGMP binding site B interact and are co-dependent of one another. To test this hypothesis two aims were constructed: **Aim 1:** To develop an S1.5 analog that utilizes both the nest and the B-site to increase S-tide activity, **Aim 2:** To explore the intricacies of these modes of activation and how they interact with each other to obtain a better understanding of the interplay between these two sites. First, based on the most potent S-tide S1.5 (YEDAEAKAKYEAEAAFFANLKLSD,  $K_a=6 \mu\text{M}$ ), two analogs were synthesized. The peptide S2.5 which lacked the amino acids LSD at the C-terminus showed a three-fold lower activation constant ( $K_a= 15 \mu\text{M}$ ), although the molecule retained its helicity as demonstrated by circular dichroism. The second analog, S3.5 contained unnatural amino acid components from a molecular modeling approach in an effort to further increase the affinity by interacting with the adjacent cGMP binding site B. However, S3.5 showed further reduction in activity with an activation constant of  $70 \mu\text{M}$ . These findings led us to conclude that the failure of the SAR approach indicates a different mode of S-tide activation as had been previously thought. Next, we investigated the role of the cGMP binding site B in the mechanism of S-tide mediated PKG I $\alpha$  activation. Co-activation assays with cGMP and S1.5 demonstrated that cGMP activation is not altered in the presence of S1.5. Furthermore, S1.5 mediated activation is negatively affected in the presence of cGMP. These results suggest that the B-site of cGMP does not positively enforce the S1.5 activation kinetics. Next, we employed the PKG I $\alpha$  mutant E292A, which cannot bind cGMP to the B-site (Moon et.al., 2018). Interestingly, this mutant retains the activation kinetics of PKG I $\alpha$  WT when activated via S1.5 and cGMP. Thus, the cGMP binding site B is not crucial in the activation mechanisms of activating PKG I $\alpha$  with cGMP. Likewise, the cGMP binding site B is not crucial in the activation mechanisms of activating PKG I $\alpha$  with S1.5. To further support these findings, the PKG I $\alpha$  mutant C42A, which showed crippled cGMP activation kinetics could be activated with S1.5 with a potency similar to wild type.

Taken together, the results in this thesis demonstrate that in contrast to the initial hypothesis the binding sites for S-tides and cGMP, although in proximity, show no experimental support of a positive interaction. These findings are significant as they reveal that S1.5 mediated activation of PKG is truly independent of cGMP, thereby providing a molecular platform for the therapeutic development of these unique peptides.

## **AKNOWLEDGEMENTS**

I would like to first express my sincere gratitude of Dr. Wolfgang Dostmann (aka Wolfie, aka Wo Do, aka Schmaltzy, aka Wolf Meister). As my advisor he went above and beyond, not only teaching me how to think critically about science but about life and how to do it with a smile the whole time. His selfless nature helped me persevere in the face of monumental tasks and when the going got tough he taught me to step back clear my head, usually with a boardgame, and approach the problem from a different angle. This is a lesson I will never forget.

I would like to thank my parents and my sister for always supporting me and listening when I need rant. I would like to thank all of my friends and family members for being my emotional support, and help along the way. I would like to thank my dog Bubba for always being there with a wiggly butt and a lot of kisses when I come home from work every day.

The University of Vermont has become my home and is filled with people that have made my goal a reality. I need to thank the pharmacology department for giving me this opportunity and helping me every step of the way. I would not have been able to do this thesis without the previous graduate students of the Dostmann lab and none more than Dr. Jessica Moon who taught me many lab techniques. Lastly I would like to thank my thesis committee; Dr. Morielli, Dr. Wellman and Dr. Freeman, who all took time out of their extremely busy schedules to be an active part of this process and helping me succeed.

## TABLE OF CONTENTS

ABSTRACT.....	i
ACKNOWLEDGEMENTS.....	ii
LIST OF TABLES.....	vii
LIST OF FIGURES.....	viii
1.0 INTRODUCTION.....	1
1.1 Genetic Overview.....	1
1.2 Pkgs Role In Smooth Muscle Relaxation.....	2
1.3 The Architecture Of Cgmp-Dependent Protein Kinase Type I.....	5
1.4 N-Terminal Dimerization Domain.....	7
1.5 Autoinhibitory Domain.....	9
1.6 Cyclic Nucleotide Binding Domain.....	9
1.7 The Catalytic Domain.....	12
1.8 The Switch Helix.....	15
1.9 Aims Of Thesis.....	18
1.10 References.....	21
2.0 MATERIALS AND MEATHODS.....	28
2.1 Protein Expression And Purification.....	28
2.1.1 Blue-White Screening.....	28
2.1.2 Bacmid Isolation.....	28
2.1.3 M13 Pcr Bacmid Analysis.....	29

2.1.4	Tranfection And First Amplification Of Baculovirus.....	31
2.1.5	Second Amplification Of Baculovirus.....	31
2.1.6	Third Amplification Of Baculovirus And Test Expression.....	32
2.1.7	Expression And Purification Of Pkg I $\alpha$ .....	33
2.2	Peptide Synthesis.....	36
2.3	Circular Dichroism Spectroscopy.....	36
2.4	P81 Phosphotransfer-Assay.....	37
2.4.1	S1.5 And Cgmp Incubation Assays & S-Tide Analog Kinetic Assays.....	38
2.4.2	Activator Combination Assays & Pkg I $\alpha$ Mutant Assays.....	39
2.5	Synthesis of P81 Phosphocellulose.....	40
2.5.1	Validation of P81 Phosphocellulose.....	42
2.6	Data Analysis.....	42
3.0	RESULTS.....	43
3.1	Protein Expression And Purification.....	43
3.2	Determination Of Optimal Activation Conditions For S-Tide Activation Of Pkg-I $\alpha$ .....	46
3.3	Comparing The Activation Kinetics Of S-Tide Analogs.....	48
3.4	Pkg I $\alpha$ Co-Activation And Activation Site Interplay.....	52
3.5	Activation Of Pkg I $\alpha$ E292a Mutant With Cgmp And S1.5.....	55

3.6	Efficacy Of S1.5 Activation Of The Pkg I $\alpha$ C42s Mutant.....	58
4.0	DISCUSSION AND FUTURE DIRECTIONS.....	61
5.0	REFERENCES.....	65

## LIST OF TABLES

Table 1.1	S-tide Names and Sequences.....	17
Table 2.1	M13 PCR Run Tables.....	30
Table 2.2	Nickle Affinity Chromatography Regeneration and Purification.....	35
Table 3.1.1	Kinetic constants derived from the nonlinear regression fit of the cGMP PKG I $\alpha$ WT prep Activation Curve.....	45
Table 3.2.1	Kinetic Constants Derived from The Activation Curves Comparing cGMP V.S. S1.5 and Pre-incubation <i>verses</i> no Pre-incubation.....	47
Table 3.3.1	Kinetic Constants Derived from the Activation Curves Comparing S1.5, S2.5, and S3.5 Activation of PKG I $\alpha$ .....	51
Table 3.4.1	Kinetic Constants Derived from the Activation Curves Comparing Co-activation of PKG I $\alpha$ with S1.5 and cGMP.....	54
Table 3.5.1	Kinetic Constants Derived from the Activation Curves Comparing Co-activation of PKG I $\alpha$ E292A with S1.5 and cGMP.....	57
Table 3.6.1	Kinetic Constants Derived from the Activation Curves Comparing cGMP and S1.5 Activation of the PKG I $\alpha$ Mutant C42S.....	60

## LIST OF FIGURES

Figure 1.1	PKG's Role in Vascular Smooth Muscle Relaxation.....	4
Figure 1.2	PKG I $\alpha$ /I $\beta$ Holoenzyme Domain Organization.....	6
Figure 1.3	Disulfide Bond at Cysteine 42 of PKG I $\alpha$ 's leucine zipper motif.....	8
Figure 1.4	The Regulatory domain of PKG I $\alpha$ .....	13
Figure 1.5	Catalytic Domain of PKA.....	14
Figure 1.6	Switch Helix Domain of PKG I $\alpha$ .....	16
Figure 2.5.1	Structure of sodium trimetaphosphate (P <sub>m3</sub> ).....	41
Figure 2.5.2	P81 Filter Production Device.....	41
Figure 3.1.1	Correlative Bradford Analysis of PKG I $\alpha$ WT Purification Fractions.....	44
Figure 3.1.2	Gel Electrophoresis of PKG I $\alpha$ WT Purification Steps.....	44
Figure 3.1.3	Test Activation of PKG I $\alpha$ Wild Type prep with cGMP.....	45
Figure 3.2.1	Activation Curves Comparing cGMP <i>verses</i> S1.5 and Pre-incubation <i>verses</i> no Pre-incubation.....	47
Figure 3.3.1	Structure of S2.5 and S3.5.....	50
Figure 3.3.2	Activation Curves Comparing the Kinetics of S1.5, S2.5, and S3.5.....	50
Figure 3.3.3	Circular Dichroism Helical Profile of S1.5 and S2.5.....	51
Figure 3.4.1	Co-Activation Curves of cGMP +S1.5 and S1.5 + cGMP.....	54

Figure 3.5.1	Co-Activation of PKG I $\alpha$ E292A with cGMP + S1.5 and S1.5 + cGMP.....	57
Figure 3.6.1	Activation Curves Comparing cGMP and S1.5 with the PKG I $\alpha$ C42S mutant V.S. cGMP and S1.5 activation of PKG I $\alpha$ WT.....	60

## 1.0 INTRODUCTION

### 1.1 Genetic Overview of PKG

Protein Kinases are a family of enzymes that are responsible for protein phosphorylation, an extremely important cellular mechanism for transmitting information through cells. The human kinome consists of over 500 known kinases split into several distinct groups (Manning et al., 2002). The cGMP-dependent protein kinase (Protein Kinase G, PKG) belongs to the AGC kinase family (Pearce et al., 2010). This family contains over 60 kinases but is named after three central members PKA, PKG, PKC (Arencibia et al., 2013). PKG, like all AGC kinases functions by transferring the  $\gamma$ -phosphate of an ATP to a serine or threonine residue of a basic substrate, making these enzymes basophilic serine/threonine kinases (Alessi et al., 1996). As the name suggests, PKG is a receptor for the second messenger 3',5'-cyclic guanosine monophosphate (cGMP). =

Increased levels of intracellular cGMP activate the kinase, thereby triggering phosphorylation. Within mammalian cells there are three PKG isoforms coded by two separate genes. The gene *prkg1* codes for PKG I which exists as two splice variants PKG I $\alpha$  and PKG I $\beta$  (Orstavik et al., 1997). The gene *prkg2* codes for the third isoform PKG II (Gamm et al., 1995).

The expression of these isoforms is tissue specific. The PKG I $\alpha$  isoform tends to be expressed in the heart, lungs, cerebellum, and dorsal ganglia regions of the brain (Hofmann et al., 1992). The PKG I $\beta$  isoform is expressed in the hippocampus and blood platelets (Geiselhoringer et al., 2004a). The expression of PKG II is widely distributed throughout the brain (de Vente et al., 2001). PKG is integral in the regulation of neuronal potentiation, platelet function and smooth muscle relaxation (Hofmann et al., 2006).

## 1.2 The Role of PKG in Smooth Muscle Relaxation

The contraction and relaxation of vascular smooth muscle is a tightly regulated system that maintains homeostasis throughout the body (Wang et al., 2015). Smooth muscle contraction is coordinated via calcium influx into the cell triggered by receptor binding or mechanical stretch stimuli. The influx of calcium results in calmodulin binding to  $\text{Ca}^{2+}$  which interacts with myosin light chain kinase (MLCK) (Kuo et al., 2015). The now active MLCK phosphorylates myosin light-chain (MLC), activating myosin ATPase. The activation of myosin ATPase initiates the crossbridge cycle and causes muscle contraction (Horowitz et al., 1996). Smooth muscle contraction is inhibited by myosin light-chain phosphatase (MLCP) which dephosphorylates the myosin (Morgado et al., 2012).

PKG is a key enzyme in smooth muscle relaxation and is the main downstream effector of nitric oxide (NO) signaling. The NO pathway is initiated by NO production in the endothelial layer of blood vessels. NO freely diffuses into the adjacent smooth muscle cells and binds soluble guanylyl cyclase (sGC). Activation of sGC causes the enzyme to convert guanosine tris-phosphate (GTP) to cGMP (Derbyshire and Marletta, 2009) (**Figure 1.1**). The increased levels of cGMP activate PKG which causes smooth muscle relaxation in several ways but mainly through a decrease in intracellular  $\text{Ca}^{2+}$  (Hofmann, 2005). Alterations of intracellular  $\text{Ca}^{2+}$  via PKG is achieved in a few ways. The first mechanism decreases intracellular  $\text{Ca}^{2+}$  through the phosphorylation of inositol triphosphate receptor-associated cGMP kinase substrate (IRAG), this forms a complex with the inositol triphosphate receptor ( $\text{IP}_3\text{R}$ ) which inhibits the flow of  $\text{Ca}^{2+}$  from the sarcoplasmic reticulum (SR) (Casteel et al., 2008). Another substrate for PKG that decreases intracellular  $\text{Ca}^{2+}$  is RGS2 (regulator of G-protein signaling 2), this is an indirect action because phosphorylation of RGS2 results in a decrease of G-protein based

IP<sub>3</sub> synthesis (Kehrl et al., 2002). The decrease in IP<sub>3</sub> reduces the activation of the IP<sub>3</sub> receptor and therefore Ca<sup>2+</sup> release (Sun et al., 2005). Phospholamban (PLN) is also phosphorylated by PKG, when PLN is phosphorylated it stops the inhibiting the SR Ca<sup>2+</sup>-ATPase (SERCA) and allows it to pump Ca<sup>2+</sup> to the SR, decreasing the level of intracellular calcium (Lalli et al., 1999).

PKG can phosphorylate K<sub>ca</sub> 1.1 channel causing a efflux of K<sup>+</sup> ions and cellular hyperpolarization which inhibits the L-type Ca<sup>2+</sup> channels from increasing intracellular calcium levels (Bolotina et al., 1994). Activation of PKG also effects phosphorylation of myosin in a more direct manner by enhancing the function of MLCP through inhibition of Ras homolog gene family member A (RhoA) and activation of Myosin phosphatase target subunit 1 (MYPT1). The phosphorylation of MYPT1 directly causes MLCP dephosphorylation of the myosin head (Wooldridge et al., 2004). Phosphorylation of RhoA inhibits the activating of an effector protein that phosphorylates the targeting region of MYPT1 that would inhibit binding to myosin and dephosphorylation. (Shin et al., 2002)

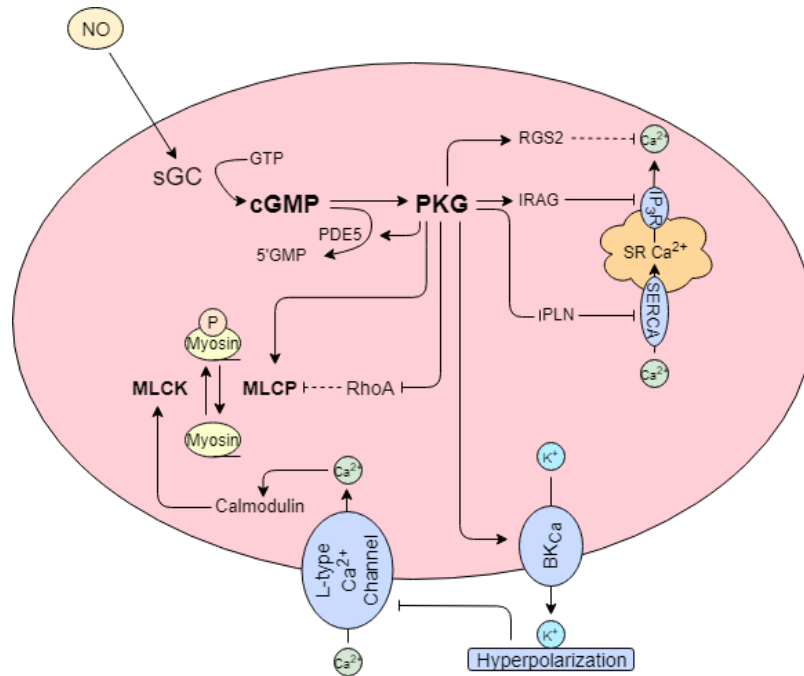


**Figure 1.1. PKG's role in vascular smooth muscle relaxation.**

The vascular smooth muscle signaling pathways controlled by PKG displayed in a simplified manner. The direct activations are depicted by solid lines and arrows, and the direct inhibitions are depicted by solid lines with solid perpendicular lines. The indirect actions are depicted by dotted lines. Abbreviations; soluble guanylyl cyclase: sGC, Phosphodiesterase 5: PDE5, Regulator of G-protein signaling 2: RGS2, inositol triphosphate receptor-associated cGMP-kinase substrate: IRAG, Phospholamban: PLN, Ras homolog gene family member A: RhoA, Myosin Light Chain Kinase and Phosphorylase: MLCK and MLCP, Calcium Activated Potassium channel: BK<sub>Ca</sub>.

### **1.3 The Architecture of cGMP- Dependent Protein Kinase Type I**

The general organization of PKG's domains is conserved amongst all isoform. PKG exists as a parallel homodimer (Huggins et al., 1994). PKG 1 $\alpha$  and PKG 1 $\beta$  consists of 671 and 686 amino acids, with molecular weights of 153 kDa and 156 kDa respectively (Wernet et al., 1989). These isoforms share sequence homology in their regulatory and catalytic domains and vary in their dimerization and autoinhibitory domains which has been shown to affect their activation and substrate targeting (Orstavik et al., 1992, 1997; Casteel et al., 2010; Qin et al., 2015; Ruth et al., 1991). Located at the N-terminus of the protein is a dimerization domain (DD) connecting the two protomers together, followed by a linker region. After the linker region there is an autoinhibitory domain (AI) (aa 1-87) connected to another linker region. The next domain is the cyclic nucleotide binding domain, consisting of two cGMP binding sites denoted as the high-affinity A-site (aa 87-211) and the low affinity B-site (aa 211-329). At the C-terminus of the B-site there is a region called the switch helix domain (SW) (aa 329-355) which interacts with the opposing protomer. Proceeding the SW is the catalytic domain (aa 358-671) (**Figure 1.2**).

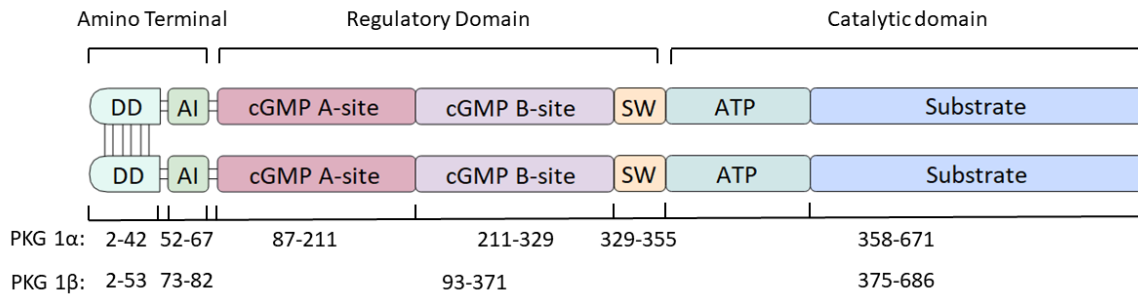


**Figure 1.2. PKG I $\alpha$ /I $\beta$  Holoenzyme Domain Organization**

Organization of the individual domains within the parallel homodimer of PKG I $\alpha$  and I $\beta$ . The dimerization domain (DD), auto-inhibitory domain (AI), High-affinity cGMP binding site (A-site), low-affinity cGMP binding site (B-site), switch helix (SW), and catalytic domain sub divided into the ATP and substrate binding regions.

#### 1.4 N-terminal Dimerization Domain

The N-terminus of PKG is home to the dimerization domain (DD) which contains a leucine zipper motif. The leucine zipper is an amphipathic, left-handed  $\alpha$ -helix of two opposing protomers that interact and joins them together (Atkinson et al., 1991; Casteel et al., 2010; Qin et al., 2015). The helices in this motif exhibit an amino acid heptad repeat (*abcdefg*) with hydrophobic residues at the *a* and *d* positions and hydrophilic residues at the *e* and *g* positions (O'Shea et al., 1991; Atkinson et al., 1991). The *a* positioned amino acid residues are either leucines or isoleucines, the *d* position can have a wider diversity of amino acids. In PKG 1 $\alpha$  there are four *d* residues that are non-hydrophobic amino acids (Phe7, Lys14, Lys28, Cys42) (Qin et al., 2015). The Cys42 residue is an integral residue in dimerization because it forms a disulfide bond with the opposing protomer (Monken and Gill, 1980; Schnell et al., 2005)(**Figure 1.3.**). The differences in the amino acid sequence in the leucine zipper of different isoforms results in alternate charge distribution, this causes them to target different substrates (Schlossman and Desch, 2009). This isoform specific leucine zipper sequence variation also results in determining their cellular localization via interaction with specific G-Kinase-anchoring proteins (GKAPs) (Casteel et al., 2008).

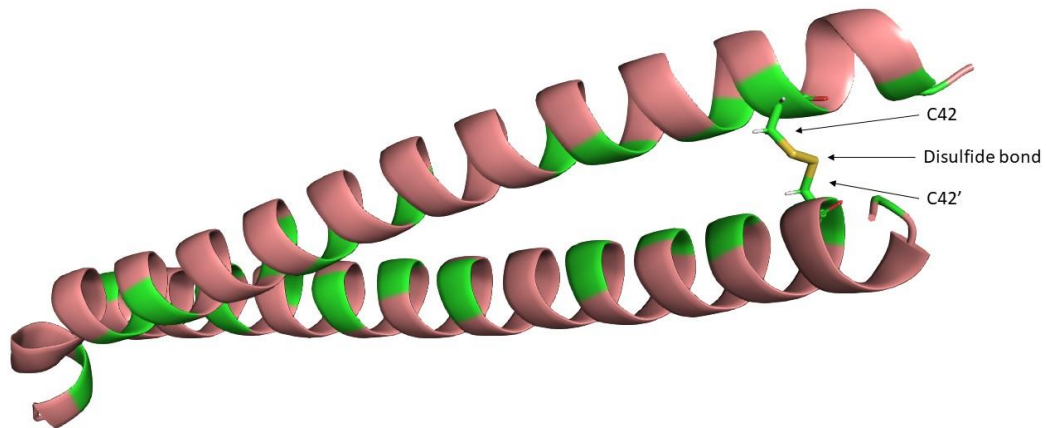


**Figure 1.3. Disulfide bond at cysteine 42 of PKG Iα's leucine zipper motif (PBD 4R4L)**

Leucine zipper interaction between two opposing protomers of PKG Iα. Highlighted is the cysteine 42 residue of both protomers which displays the disulfide bond formed between the two when the protein is dimerized.

## **1.5 Autoinhibitory Domain**

Following the dimerization domain is the auto inhibitory domain (AI) of PKG. The AI is found at amino acid 51-68 and 66-83 in the 1 $\alpha$  and 1 $\beta$  isoforms, respectively. This region of the enzyme has been determined to be an important part of PKG activation. In its inactive form the AI acts as a pseudo substrate for the catalytic domain causing PKG to adopt a tightly inhibited confirmation (Francis et al., 1996). The AI residues responsible for this autoinhibition are a glycine at residue 62 in PKG 1 $\alpha$  and an alanine at residue 77 in PKG 1 $\beta$  found in the sequence XISAEP (Kemp et al., 1988; Francis et al., 1996). The precise mechanism of this inhibition has remained elusive, but it is most likely through the binding of the phosphate acceptor site of the catalytic region preventing substrate phosphorylation, a mechanism closely homologous to PKA (Francis et al., 1996). This inhibition mechanism is supported by the generation of a PKG I $\alpha$  mutant with a truncation mutation to Arg77, the resulting enzyme was constitutively active (Heil et al., 1987; Landgraf et al., 1990; Scholten et al., 2007). Within the AI it has also been seen that autophosphorylation can occur in the presence of both cAMP and cGMP at Thr58, this is believed to cause ubiquitination and turnover of PKG I $\alpha$  (Takioe et al., 1983; Atiken et al., 1984; Dey et al., 2009).

## **1.6 Cyclic Nucleotide Binding Domain**

The cyclic nucleotide binding domain of PKG is responsible for regulating the activity of the enzyme. This domain in both PKG I $\alpha$  and I $\beta$  is structurally identical containing two consecutive cyclic nucleotide binding sites per protomer. Despite having the same structure PKG I $\alpha$  and PKG I $\beta$  have different activation kinetics. It has been shown that there is a 10-20 fold difference in their cGMP activation constants ( $K_a$ ), PKG

I $\alpha$  has a  $K_a$  of about 100 nM, whereas PKG I $\beta$  has a  $K_a$  of 1-2  $\mu$ M (Ruth et al., 1991). This variance in activation kinetics is, thought to stem from the differences found in the dimerization domain (DD) and the autoinhibitory domain (AI) as well (Ruth et al., 1997).

Within this domain the two cGMP binding sites have very different kinetics. The A-site is known as the high-affinity binding site and binds cGMP with a higher affinity than the B-site (low-affinity binding site) with binding affinities of 17 nM and 100-150nM cGMP, respectively (Corbin et al., 1986). The amino acid residues responsible for binding cGMP are highly conserved so it is interesting that these two sites display different binding kinetics for cGMP. The difference may be a result of the theory of the B-site acting more as a selectivity filter for cGMP. It was initially thought that the selectivity filter for cGMP over cAMP was a threonine found in both sites in both isoforms Thr177/192 and Thr301/316 PKG I $\alpha$  and I $\beta$  respectively (Kim et al., 2011). After further investigation of an isolated A-site it was determined that the binding constants ( $K_D$ ) were 12 and 27 nM for cGMP and cAMP respectively showing that there is poor selectivity via the previous mechanism. It was demonstrated that the cyclic nucleotide selectivity is caused by the B-site at Arg281/296 which interact with O6 and N7 on the guanine, in the A-site the equivalent residue is Leu155/170 (Huang et al., 2014; Kim et al., 2011, 2016).

The holoenzyme crystal structure has yet to be solved, we only have crystal structures of isolated DD and regulatory domain and therefore do not have a structure detailing the complex interaction of the cyclic nucleotide binding sites, the N-terminal domains and the catalytic domain.

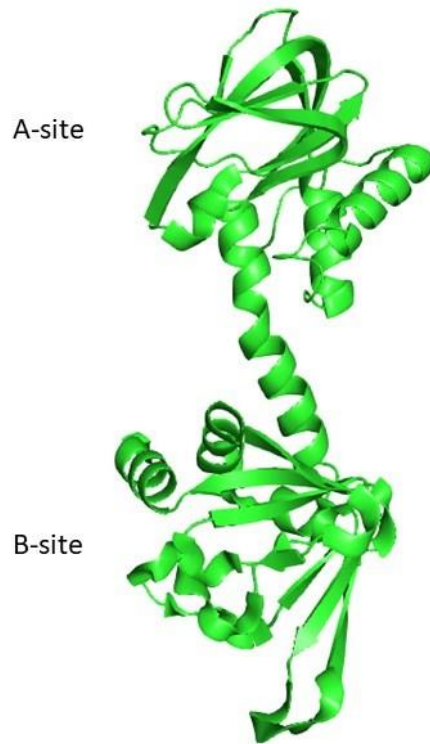


**Figure 1.4 The Regulatory Domain of PKG I $\alpha$  (PDB 3SHR)**

Displayed above is the regulatory domain of PKG I $\alpha$  consisting of amino acids 77-326. The domain is split into the high affinity cGMP binding A-site and the low affinity cGMP binding B-site.

## 1.7 The Catalytic Domain

The C-terminal domain of PKG is its catalytic domain (PKG 1 $\alpha$  aa 360-671, PKG 1 $\beta$  aa 375-686) responsible for binding substrate/ATP and catalyzing the phosphorylation reaction. Like all AGC kinases PKG transfers the  $\gamma$ -phosphate of ATP to a serine or threonine residue of the basic substrate (Alessi et al., 1996). Due to the lack of complete crystal structures of PKG the exact 3D conformation of this region is unknown. Therefore, we rely on biochemical data and the known structures of PKA and its sequence homology models of PKG. The crystal structures of 14 different AGC kinases show a conserved fold in this domain (Pearce et al., 2012; Taylor et al., 2005). The fold as seen in PKA show the catalytic subunit is divided into a small N-terminal lobe (N-lobe), responsible for binding ATP, and a large C-terminal lobe (C-lobe), containing the catalytic and the substrate binding region (Kim et al., 2007)(**Figure 1.5**). Within the N-lobe there is a loop containing several glycine residues that bind the  $Mg^{2+}$  binding loop and ATP. This region arranges the ATP's  $\gamma$ -phosphate into the catalytic site for the phosphoryl transfer reaction. The N-lobe also functions to help create the active site by coordinating components of the C-lobe. The C-lobe is responsible for a majority of the reaction catalyzing residues. The C-lobe contains a catalytic loop containing an aspartate which deprotonates the substrates serine or threonine residue.  $Mg^{2+}$  ions are positioned via N-lobe residues and the activation loops DFG motif. A threonine residue (Thr197) in the activation loop is phosphorylated causing a conformational change aligning the N-lobe, the activation loop and substrate binding sites to their active positions (Bastidas et al., 2013; Smith et al., 1999; Steichen et al., 2012). It has been shown that Thr516 on PKG I $\alpha$  serves as the equivalent to Thr197 of PKA (Feil et al., 1995). The lack of PKG holoenzyme crystal structure leaves some uncertainty about the structural details of its

catalytic domain but sequence homology with PKA allows us to make well educated assumptions that suggest it functions much like the mechanisms above.

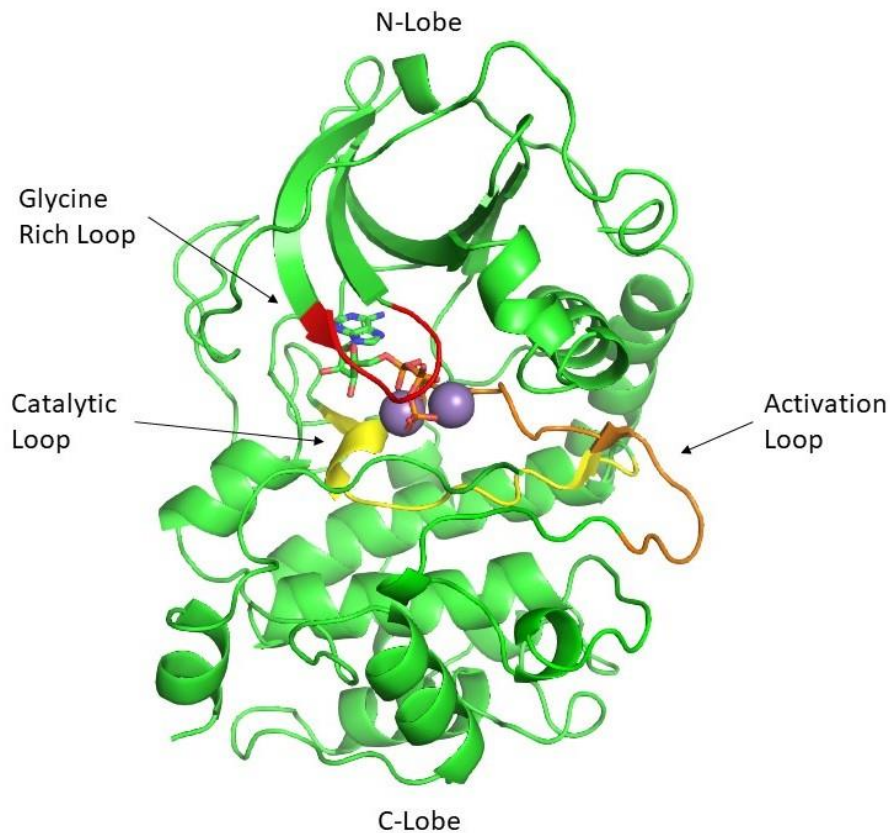


**Figure 1.5. Catalytic domain of PKA**

Displayed is the catalytic domain of PKA which is structurally homologous to all AGC kinases and therefore is relevant as a model for the catalytic domain of PKG. The model displays the N-lobe and C-lobe of the domain top and bottom respectively. The catalytically relevant loops are color coded. The red loop represents the glycine rich loop. The yellow loop represents the catalytic loop. The orange loop represents the activation loop. The magenta loop represents the P + 1 loop. Within the N-lobe are two  $Mg^{2+}$  ions and bound ATP, blue and salmon respectively.

## 1.8 The Switch Helix

Directly following the B-site a domain known as the switch helix (SW) was discovered through x-ray crystallography by Osborne et al. (2011) (**Figure 1.4**). The SW is an  $\alpha$ -helix located at the junction of the regulatory and catalytic domains, amino acids 329-355 of PKG I $\alpha$ . The C-terminus of the helical switch domain consists of a series of hydrophobic residues (AAFFANL) called the “knob” (aa 350-345) which interacts with complementary hydrophobic residues of the phosphate binding cassette (PBC), the N<sub>3</sub>A,  $\alpha$ B and  $\beta$ 6 motifs from the B-site of the opposing protomer, this is called the “nest” (Osborne et al., 2011; Moon et al., 2013). Including the leucine zipper of the DD this SW domain represents one of only two sites of interprotomer interaction and communication.

The effect of the switch helix on PKG activation was explored further by Moon et al. (2015) who found that a synthetic peptide of the same sequence of the alpha helix from the SW (aa 329-358) known as S-tide 1.1 (S1.1) activated PKG I $\alpha$  independently of cGMP (**Table 1.1**). Following this discovery, a series of synthetic S-tides were created to determine the essential amino acid sequence for activation. The C-terminal amino acids were analyzed for significance, removing 3 amino acids at a time two S-tides were created and showed that the first three could be removed without change in activity (S1.2), however the subsequent deletion (S1.3) resulted in an inactive peptide due to the absence of the knob residues. The N-terminus was then investigated in the same manner resulting in two S-tides with 3 and 6 amino acids removed S1.4 and S1.5 respectively. The truncations resulted in increased activity with as low as 3  $\mu$ M S1.5 (Moon et al., 2015). This effect is only observed in PKG I $\alpha$  and not PKG I $\beta$  and presents the possibility of a PKG I $\alpha$  selective novel drug target.

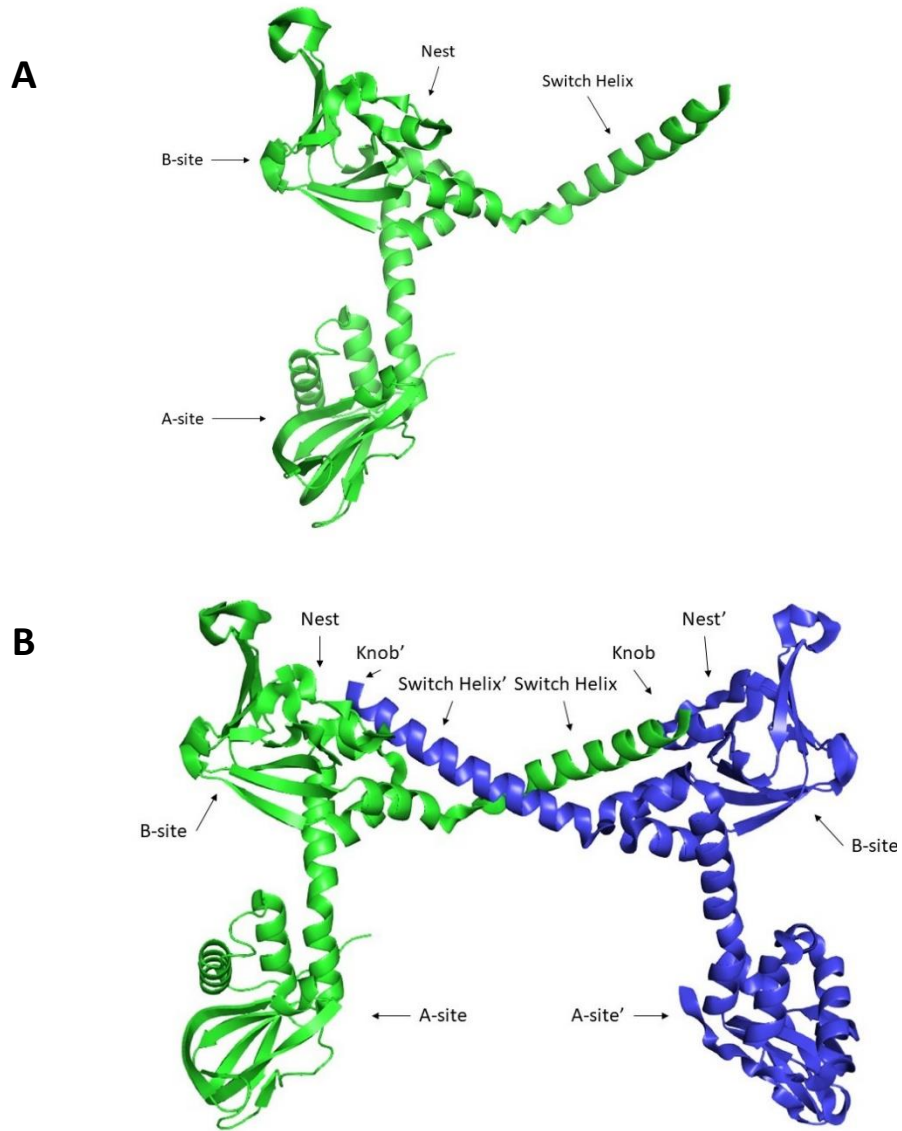


**Figure 1.6. Switch helix domain of PKG I $\alpha$  (PDB 3SHR)**

Pictured is the switch helix domain of PKG I $\alpha$  as well as the cGMP A & B site of the regulatory domain. The two opposing protomers are denoted by green and purple and the various subparts of each domain are labeled with red arrows. A; represents one protomer of the SW and regulatory domain whereas B represents the interaction of the two opposing protomers

<i>Name</i>	<i>Sequence</i>	$K_a(\mu M)$	$n_H$
<i>S1.1</i>	Ac-DVSNKAYEDAEAKAKYEAAFFANLKLSD-NH <sub>2</sub>	35 ±4	2.2 ±0.4
<i>S1.2</i>	Ac-DVSNKAYEDAEAKAKYEAAFFANLK-NH <sub>2</sub>	35 ±4	3.6 ±0.8
<i>S1.3</i>	Ac-DVSNKAYEDAEAKAKYEAAA-NH <sub>2</sub>	-	-
<i>S1.4</i>	Ac-NKAYEDAEAKAKYEAAFFANLKLSD-NH <sub>2</sub>	12 ±1	1.9 ±0.6
<i>S1.5</i>	Ac-YEDAEAKAKYEAAFFANLKLSD-NH <sub>2</sub>	3 ±1	2.4 ±0.6
<i>S1.9</i>	Ac-EDAEAKAKYEAAFFANLKLSD-NH <sub>2</sub>	43± 5	2.7 ±0.7
<i>S1.10</i>	Ac-DAEAKAKYEAAFFANLKLSD-NH <sub>2</sub>	45±4	3.0± 0.7
<i>S1.11</i>	Ac-AEAKAKYEAAFFANLKLSD-NH <sub>2</sub>	-	-
<i>S1.6</i>	Ac-DVSNKAYEDAEAKAKYEAAAAANLKLSD-NH <sub>2</sub>	-	-
<i>S1.7</i>	Ac-ALKSENYADKVEFKDAKYEASALANEFADA-NH <sub>2</sub>	-	-

**Table 1.1. S-Tide Name and sequence.**

The name of the sequences are listed in order of development on the left of the table followed by their corresponding sequences, activation constant ( $K_a$ ) in  $\mu M$  concentration, and Hill coefficient ( $n_H$ ). The peptide sequences are aligned based on the position of the knob sequence.

## **1.9 Aims of Thesis**

The following central hypothesis and specific aims were constructed to explore the structure activity relationship of S-tide mediated activation with respect to the cGMP B-site.

**Hypothesis: The binding site for the S-tides (nest) and the cGMP binding site B interact and are co-dependent of one another.**

**Aim 1: To develop an S1.5 analog that utilizes both the nest and the B-site to increase S-tide activity.**

To test this, we will create two peptides derivatives of S1.5 with sequential C-terminal modifications to probe the low affinity cGMP B-site. The first of the two peptides will be a three amino acid truncation that is necessary for further peptide modification. The second will consist of the truncated peptide with the addition of a cysteamine linker that should reach the B-site. The activity of these peptides will be tested via kinase assays.

**Aim 2: To explore the intricacies of cGMP and S-Tide mediated activation and how they interact with each other to obtain a better understanding of the interplay between these two sites.**

To test this, we will use of activator combination kinase assays and mutant forms of PKG allowing us to create a kinetics based model of the activation of each of these sites. The combination assays will consist of a constant concentration of cGMP with dose response concentrations of S1.5 and constant concentration of S1.5 with dose response concentrations of cGMP. To test the direct effect of the B-site interaction with the SW we will be testing the B-site knock out mutant (E292A). To test the overall similarity in

activation mechanism we will employ the C42S mutant which has a documented degradation of cGMP activation.

The aim of this thesis serves to explore the structure to function relationship of the switch helix domain of PKG. The previous work of the Dostmann laboratory uncovered the structure of the switch helix domain and went further to discover the unique ability of synthetic peptides, derived from the switch helix, to activate the holoenzyme and establish the possibility for a novel drug target not before observed. This preliminary work warranted further exploration into the mechanics of this unique property of PKG. It was necessary to test the effects preincubation had on S-tide activation and PKG with cGMP due to the slow binding kinetics of S1.5 and the need to establish standard assay conditions. To further explore the possibilities of S-tides new derivatives of the most potent S-tide (S1.5) were created via molecular modeling with the rational of creating a peptide that would interact with the adjacent cGMP B-site of PKG I $\alpha$ . The possible interaction would strengthen the activation kinetics of the S-tides. This portion of the thesis demanded that we construct intermediary S1.5 analogs to test the kinetic effect of removing the three c-terminal amino acids of S1.5 and the addition of a linker resulting in the new S2.5 and S3.5 peptides. To test their role, we employed secondary structure analysis via, circular dichroism spectroscopy, as well as kinetic assays. We hypothesized that the subtraction of these amino acids would not have a significant effect and if they did it would be due to a loss of helicity.

Since the switch helix binding site shares amino acids with the phosphate binding cassette (PBC), the N3A,  $\alpha$ B and  $\beta$ 6 motifs from the B-site prompted us to investigate the interplay between cGMP and S-tide activation. We hypothesized that the mechanism of activation was linked. To test this, we employed activator combination assays with PKG

I $\alpha$  WT as well as the mutant PKG I $\alpha$  E292A (B-site knock-out). To test the similarity of the two forms of activation we employed the mutant PKG I $\alpha$  C42S which has documented degradation of cGMP activation. This work was conducted to further our understanding of the switch helix and its mechanism of action. The results of this endeavor serve as a base for further research into the structure and function of PKG and its exploitation as a potential novel drug target.

## 1.10 References

Adler, A.J., Greenfield, N.J., Fasman, G.D. (1973). Circular dichroism and optical rotatory dispersion of proteins and polypeptides. *Methods Enzymol* 27, 675.

Alessi, D.R., Caudwell, F.B., Andjelkovic, M., Hemmings, B.A., and Cohen, P. (1996). Molecular Basis for the Substrate specificity of protein kinase B; comparison with MAPKAP kinase-1 and p70 S6 kinase. *FEBS Lett* 399, 333-338.

Arencibia, J, Pastor-Flores, D., Bauer A., Schulze, J., Bondi, R. (2013). AGC protein kinases: From structural mechanism of regulation to allosteric drug development for the treatment of human diseases. *Biochimica et Biophysica Acta (BBA) - Proteins and Proteomics*, Vol 1834, Issue 7, 1302-1321.

Aitken, A., Hemmings, B.A., and Hofmann, F. (1984). Identification of the residues on cyclic GMP-dependent protein kinase that are autophosphorylated in the presence of cyclic AMP and cyclic GMP. *Biochim Biophys Acta* 790, 219-225.

Atkinson, R.A., Saudek, V., Huggins, J.P., and Pelton, J.T. (1991). <sup>1</sup>H NMR and circular dichroism studies of the N-terminal domain of cyclic GMP dependent protein kinase: a leucine/ isoleucine zipper. *Biochemistry* 30, 9387-9395.

Bastidas, A.C., Deal, M.S., Steichen, J.M., Guo, Y., Wu, J., and Taylor, S.S. (2013). Phosphoryl transfer by protein kinase a is captured in a crystal lattice. *J Am Chem Soc*, 135(12):4788-98.

Bolotina, V.M., Najibi, S., Palacino, J.J., Pagano, P.J., and Cohen, R.A. (1994). Nitric oxide directly activates calcium-dependent potassium channels in vascular smooth muscle. *Nature* 368, 850-853.

Casteel, D.E., Zhang, T., Zhuang, S., and Pilz, R.B. (2008). cGMP-dependent protein kinase anchoring by IRAG regulates its nuclear translocation and transcriptional activity. *Cellular signaling* 20, 1392-1399.

D. E. Casteel, E. V. Smith-Nguyen, B. Sankaran, S. H. Roh, R. B. Pilz, and C. Kim. A crystal structure of the cyclic gmp-dependent protein kinase I beta dimerization/docking

domain reveals molecular details of isoform-specific anchoring. *J Biol Chem*, 285(43):32684-32688, 2010.

Corbin, J.D., Og Reid, D., Miller, J.P., Suva, R.H., Jastorff, B., and Doskeland, S.O. (1986). Studies of cGMP analog specificity and function of the two intrasubunit binding sites of cGMP-dependent protein kinase. *J Bio Chem* 261, 1208-1214.

Derbyshire, E.R., and Marletta, M.A. (2009). Biochemistry of soluble guanylate cyclase. *Handb Exp Pharmacol*, 17-31.

de Vente, J., Asan, E., Gambaryan, S., Markerink-van Ittersum, M., Axer, H., Gallatz, K., Lohmann, S.S., and Palkovits, M. (2001). Localization of the cGMP-dependent protein kinase type II in rat brain. *Neuroscience* 108, 27-49.

Dey, N.B., Busch, J.L., Francis, S.H., Corbin J.D., and Lincon T.M. Cyclic gmp specifically suppresses type-Ialpha cgmp-dependent protein kinase expression by ubiquitination. *Cell Signal*, 21(6):859-66, 2009.

Orstavik, S., Natarajan, V., Tasken, K., Jahnsen, T., and Sandberg, M. (1997). Characterization of the human gene encoding the type I alpha and type I beta cGMP-dependent protein kinase (PRKG1). *Genomics* 42, 311-318.

Francis, S.H., Smith, J. A., Colbran, J. L., Grimes, K., Walsh, K.A., Kumar, S., and Corbin, J.D. Arginine 75 in the pseudosubstrate sequence of type I beta cGMP-dependent protein kinase is critical for autoinhibition, although autophosphorylated serine 63 is outside this sequence. *J Biol Chem*, 271(34):20748-55, 1996.

Feil, R., Kellermann, J., and Hofmann, F. (1995). Functional cGMP-dependent protein kinase is phosphorylated in its catalytic domain at threonine-516. *Biochemistry* 34, 13152-13158.

Gamm, D.M., Francis, S.H., Angelotti, T.P., Corbin, J.D., and Uhler, M.D. (1995). The type II isoform of cGMP-dependent protein kinase is dimeric and possesses regulatory and catalytic properties distinct from the type I isoforms. *J Biol Chem* 270, 27380-27388.

Heil, W.G., Landgraf, W., Hofmann, F. A catalytically active fragment of cGMP-dependent protein kinase. Occupation of its cGMP-binding sites does not affect its phosphotranferase activity. *Eur J Biochem*, 168(1):117-21, 1987.

Hofmann, F., Dostmann, W., Keilbach, A., Landgraf, W., Ruth, P. (1992). Structure and physiological role of cGMP-dependent protein kinase. *Biochim Biophys Acta*; 1135(1): 51-60.

Hofmann, F., Feil, R., Kleppisch, T., and Schlossmann, J. (2006). Function of cGMP-dependent protein kinases as revealed by gene deletion. *Physiological reviews* 86, 1-23.

Hofmann, F. (2005). The biology of cyclic GMP-dependent protein kinases. *J Biol Chem* 280, 1-4.

Horowitz, A., Menice, C.B., Laporte, R., and Morgan, K.G. (1996). Mechanisms of smooth muscle contraction. *Physiol Rev* 76, 967-1003.

Huang, G.Y., Kim, J.J., Reger, A.S., Lorenz, R., Moon, E.W., Zhao, C., Casteel, D.E., Bertinetti, Vanshouwen, B., Selvaratnam, R., Pflugrath, J.W., Sankaran, B., Melacini, G., Herberg, F.W., and Kim, C. (2014). Structural basis for cyclic-nucleotide selectivity and cGMP-selective activation of PKG I. *Structure*, 22(1):116-24.

Huggins, J.P., Ganzhorn, A.J., Saudek, V., Pelton, J.T., and Atkinson, R.A. (1994). Stimulation of cGMP-dependent protein kinase I alpha by a peptide from its own sequence. An investigation by enzymology, circular dichroism and <sup>1</sup>H NMR of the activity and structure of cGMP-dependent dependent protein kinase I alpha-(546-576)-peptide amide. *European journal of biochemistry / FEBS* 221, 581-593.

Kehrl, J.H., Sinnarajah, S. (2002). RGS2: a multifunctional regulator of G-protein signaling. *Int J Biochem Cell Biol*: 34(5): 432-8.

Kemp, B.E., Cheng, H.C., Walsh, D.A. Peptide inhibitors of camp-dependent protein kinase. *Methods Enzymol*, 159:173-83, 1988.

Kim, C., Cheng, C.Y., Saldanha, S.A., and Taylor, S.S. (2007). PKA-I holoenzyme structure reveals a mechanism for cAMP- dependent activation. *Cell* 130, 1032-1043.

Kim, J.J., Casteel, D.E., Huang, G., Kwon, T.H., Ren, R.K., Zwart, P., Headd, J.J., Brown, N.G., Chow, D.C., Palzkill, T., and Kim, C. (2011). Co-crystal structures of PKG Ibeta (92-227) with cGMP and cAMP reveal the molecular details of cyclic nucleotide binding. *PLoS One* 6, e18413.

Kim, J.J., Lorenz, R., Arold, S.T., Reger, A.S., Sankaran, B., Casteel, D.E., Herberg, F.W., and Kim, C. (2016). Crystal structure of PKG I: cGMP complex reveals a cGMP-mediated dimeric interface that facilitates cGMP-induced activation, *Structure*, 24(5):710-20.

Kuo, I.Y., Ehrlich, B.E. (2015). Signaling in muscle contraction. *Cold Spring Harb Perspect Biol*: 7(2):a006023.

Lalli, M.J., Shimizu, S., Sutliff, R.L., Kranias, E.G., and Paul, R.J. (1999). [Ca<sup>2+</sup>]I homeostasis and cyclic nucleotide relaxation in aorta of phospholamban-deficient mice. *Am J Physiol* 277, H963-970

Landgraf, W., Hofmann, F., Pelton, J.T., Huggins, J.P. Effects of cyclic gmp on the secondary structure of cyclic gmp dependent protein kinase and analysis of the enzyme's amino terminal domain by far-ultraviolet circular dichroism. *Biochemistry*, 29(42):9921-8, 1990.

Manning, G., Whyte, D. B., Martinez, R., Hunter, T., Sadarsanam, S. (2002). The protein kinase complement of the human genome. *Science*: 298(5600): 1912-34.

Morgado, M., Cairrao, E., Santos-Silva, A.J., and Verde, I. (2012). Cyclic nucleotide-dependent relaxation pathways in vascular smooth muscle. *Cellular and molecular life sciences : CMLS* 69, 247-266.

Monken, C.E., and Gill, G.N. (1980). Structural analysis of cGMP-dependent protein kinase using limited proteolysis. *J Bio Chem* 255, 7067-7070.

Moon, T.M., Osborne, B.W., and Dostmann, W.R. (2013). The switch helix: A putative combinatorial relay for inter protomer communication in cGMP-dependent protein kinase. *Biochin Biophys Acta* 1834(7): 1346-1351.

Moon, T.M., Tykocki, N.R., Sheehe, J.L., Osborne, B.W., Tegge, W., Brayden, J.E., and Dostmann, W.R. (2015). Synthetic peptides as cGMP-independent activators of cGMP-dependent protein kinase I $\alpha$ . *Chem Bio*, 22(12): 1653-1661.

O'Shea, E.K., Klemm, J.D., Kim, P.S., and Alber, T. (1991). X-ray structure of the GCN4 leucine zipper, a two-stranded, parallel coiled coil. *Science* 254, 539-544.

S. Orstavik, M. Sandberg, D. Berube, V. Natarajan, J. Simard, U. Walter, R. Gagne, V. Hansson, and T. Jahnsen. Localization of the human gene for the type i cyclic gmp-dependent protein kinase to chromosome 10. *Cytogenet Cell Genet*, 59(4):270-3, 1992.

S. Orstavik, V. Natarajan, K. Tasken, T. Jahnsen, and M. Sandberg. Characterization of the human gene encoding the type i alpha and type i beta cgmp- dependent protein kinase (prkg1). *Genomics*, 42(2):311-8, 1997.

Osborne, B.W., Wu, J., McFarland, C.J., Nickl, C.K., Sankaran, B., Casteel, D.E., Woods, Jr., Kornev, A.P., Taylor, S.S., Dostmann, W.R. (2011). Crystal structure of cGMP-dependent protein kinase reveals novel site of interchain communication. *Structure*, 19(9):1317-27.

Pearce, L.R., Komander, D., and Alessi, D.R. (2010). The nuts and bolts of the AGC protein kinases. *Nat Rev Mol Cell Biol* 11, 9-22.

L. Qin, A. S. Reger, E. Guo, M. P. Yang, P. Zwart, D. E. Casteel, and C. Kim. Structures of cgmp-dependent protein kinase (pkg) i alpha leucine zippers reveal an interchain disulfide bond important for dimer stability. *Biochemistry*, 54(29): 4419-22, 2015.

P. Ruth, W. Landgraf, A. Keilbach, B. May, C. Egleme, and F. Hofmann. The activation of expressed cgmp-dependent protein kinase isozymes i alpha and i beta is determined by the different amino-termini. *Eur J Biochem*, 202(3): 1339-44, 1991.

Ruth, P., Pfeifer, A., Kamm, S., Klatt, P., Dostmann, W.R., and Hofmann, F. (1997). Identification of the amino acid sequences responsible for the high affinity activation of cGMP kinase I alpha. *J Bio Chem* 272, 10522-10528.

Schlossmann, J., Desch, M., cgk substrates. *Handb Exp Pharmacol*, (191): 163-93, 2009.

Schnell, J.R., Zhou, G.P., Zweckstetter, M., Rigby, A.C., and Chou, J.J. (2005). Rapid and accurate structure determination of coiled-coil domains using NMR dipolar couplings: application to cGMP-dependent protein kinase I alpha. *Protein Sci* 14, 24141-2428

Shin, H.M., Je, H.D., Gallant, C., Tao, T.C., Hartshorne, D.J., Ito, M., and Morgan, K.G. (2002). Differential association and localization of myosin phosphatase subunits during agonist-induced signal transduction in smooth muscle. *Circ Res* 90, 546-553.

Sun, X., Kaltenbronn, K.M., Steinberg, T.H., and Blumer, K.J. (2005). RGS2 is a mediator of nitric oxide action on blood pressure and vasoconstrictor signaling. *Mol Pharmacol* 67, 631-639.

Scholten, A., Fuss, H., Heck, A.J., Dostmann, W.R. The hinge region operates as a stability switch in cgmp-dependent protein kinase I alpha. *FEBS J*, 274 (9):2274-86, 2007.

Smith, C.M., Radzio-Andzelm, E., Madhusudan, Akamine, P., and Taylor, S.S. (1999). The catalytic subunit of cAMP-dependent protein kinase: prototype for an extended network of communication. *Prog Biophys Mol Biol* 71, 313-341.

Steichen, J.M., Kuchinskas, M., Keshwani, M.M., Yang, J., Adams, J.A., Taylor, S.S. (2012). Structural basis for the regulation of protein kinase a by activation loop phosphorylation. *J Bio Chem*, 287(18):14672-80.

Takio, T., Smith, S.B., Walsh K.A., Krebs, E.G., and Titani, K., Amino acid sequence around a "hinge" region and its "autophosphorylation" site in bovine lung cgmp-dependent protein kinase. *J Bio Chem*, 258(9): 5531-6, 1983.

Taylor, S.S., Kim, C., Vigil, D., Haste, N.M., Yang, J., Wu, J., and Anand, G.S. (2005). Dynamics of signaling by PKA. *Biochim Biophys Acta* 1754, 25-37.

Wang, G., Jacquet, L., Karamariti, E., Xu, Q. (2015). Origin and differentiation of vascular smooth muscle cells. *J Physiol*: 593(14):3013-30.

Wooldridge, A.A., MacDonald, J.A., Erdodi, F., Ma, C., Borman, M.A., Hartshorne, D.J., and Haystead, T.A. (2004). Smooth muscle phosphatase is regulated in vivo by exclusion of phosphorylation of threonine 696 of MYPT1 by phosphorylation of Serine 695 in response to cyclic nucleotides. *J Biol Chem* 279, 34496-34504.

Wernet, W., Flockerzi, V., and Hofmann, F. (1989). The cDNA of the two isoforms of bovine cGMP-dependent protein kinase. *FEBS letters* 251, 191-196.

## **2.0 MATERIALS AND METHODS**

### **2.1 Protein Expression and Purification**

#### **2.1.1 Blue-White Screening**

Expression of recombinant wild type and mutant bovine PKG I $\alpha$  was accomplished using the insect cell (Sf9) Bac to Bac baculovirus expression system (Invitrogen). First the cDNA coding for the PKG variants was transposed from pFAST Bac HTA into bacmid. Approximately 50 ng of the pFAST Bac HTA containing the construct was added to chemically competent DH10 Bac *E.coli* cells. The cells were heat shocked at 42<sup>o</sup> C for 30 seconds to allow the plasmid to enter the cells. 100  $\mu$ L of Luria medium (Luria-Bertani or LB) was added and incubated at 37<sup>o</sup>C for 5 hours in the shaker at 220 rpm. KGTIX plates were prepared with LB agar; 50  $\mu$ g/mL kanamycin; 7 $\mu$ g/mL gentamicin; 10 $\mu$ g/mL tetracycline; 40  $\mu$ g/mL isopropyl  $\beta$ -D-1-thiogalactopyranoside (IPTG), and 2.4 mg of X-gal (on the surface). The *E. coli* were plated on a KGTIX plate and incubated at 37<sup>o</sup>C for 24 hours, followed by 4<sup>o</sup>C incubation to develop blue or white color depending on disruption of LacZ gene. Typically, white colonies were picked and re-streaked onto two separate KGTIX plates. This procedure was repeated until well separated single white colonies could be harvested for bacmid isolation.

#### **2.1.2 Bacmid Isolation**

Following blue-white screening, the Bacmid DNA was harvested from a single colony that was expressing the white phenotype which meant the gene was transposed into the gene that codes for  $\beta$ -galactosidase which would normally break down the

galactose from the plate and turn the colony blue. A white colony from each re-streak was harvested and suspended in 6 mL of LB containing 50 µg/ mL kanamycin and 7 µg/ mL gentamicin. The colonies were grown for 16 hours at 37°C and 220 rpm in the shake incubator. The tubes were centrifuged at 3000xg for 5 minutes, the supernatant was discarded, and the resulting pellet was resuspended in 300 µL of Quiagen Buffer P1 (50 mM Tris-HCL, 10 mM EDTA, 50-100 µg/ mL RNase A, pH 8.0). The solution was transferred to a 1.5 mL Eppendorf tube, 250 µL of Quiagen Buffer P2 (200mM NaOH, 1% SDS and LyseBlue indicator) was added and if lysis occurred the solution would turn blue. 350µL of Quaigen Buffer N3 (4.2 M guanidine hydrochloride (GuHCL), 0.9 M potassium acetate, pH 4.8) was added. The tubes were then centrifuged for 20 minutes at 15,000xg to remove cellular debris, the supernatant was transferred to a 2 mL tube with 800µL of 100% isopropanol, the solution was mixed via inversion, and the tubes were stored at -20°C for up to a month. The samples were then centrifuged at 15,000xg at 4°C for 30 minutes. The supernatant was decanted, and 7 washes were conducted to remove any remaining salt by adding 1mL of ice cold 70% ethanol to each tube and incubated for 10 minutes at 4°C, followed by 15,000xg centrifugation at 4°C for 10 minutes. The supernatant was then decanted, and the pellet was air dried. The pellet was rehydrated with 200 µL of sterile ddH<sub>2</sub>O and stored overnight at 4°C. The concentration was determined by Nanodrop® spectrophotometry 260/280 nm and corrected to 500 ng/µL.

### **2.1.3 M13 PCR Bacmid Analysis**

Following bacmid isolation, it was necessary to determine if the gene of interest was inserted into the *E.coli*, M13 PCR was employed for this determination. Each PCR

reaction had a total volume of 50  $\mu$ L containing 150 ng of the bacmid, DreamTaq, 200nM M13 forward primer (CCCAGTCACGACGTTGTAAAACG), 200nM M13 reverse primer (AGCGGATAACAATTTTCACACAGG), and ddH<sub>2</sub>O. The reactions were mixed and then run in the thermocycler with temperatures and times determined based on the primers and the DreamTaq DNA polymerase (Fisher scientific) (**Table. 3.1**). Following the PCR, a 1% agarose DNA gel (Ultrapure agarose by Invitrogen) containing SYBR Safe stain (Thermo scientific) was run with 20  $\mu$ L of each reaction and 5  $\mu$ L of a 1Kb DNA ladder (BioLabs). The gel was run in the dark in order to preserve the florescent dye at 100 volts for 45 minutes. the resulting band was the ladder equivalent of 2430 base pairs + the inserted genes length, approximately 2,013 base pairs for PKG I $\alpha$ .

step	Stage	temperature	Time (min)
1	Hot start	95 <sup>o</sup> C	1:30
2	Denature	95 <sup>o</sup> C	0:45
3	Annealing	50 <sup>o</sup> C	0:45
4	Extension	68 <sup>o</sup> C	5:00
5	Cycle	To stage 2, repeat 30x	-
6	Final extension	68 <sup>o</sup> C	7:00
7	Storage	4 <sup>o</sup> C	Forever

**Table 2.1. M13 PCR run table**

The sequence of events during M13 PCR with the corresponding temperatures and times.

#### **2.1.4 Transfection and First Amplification of Baculovirus**

Once it was determined that the gene of interest was inserted into bacmid, Sf9 cells were transfected to produce baculovirus. Under sterile conditions, 2 mL of Sf9 cells at a concentration of  $0.5 \times 10^6$  cells/mL in unsupplemented Sf900 III medium (Thermo scientific) were added to each well of a 6 well plate. The cells were allowed to adhere for 30 minutes, followed by a media change with new unsupplemented Sf900 III medium (Thermo scientific). The plate was constructed with a duplicate series of the experimental conditions; control (0  $\mu$ g), 1  $\mu$ g, and 2  $\mu$ g of a single Bacmid. Tubes were prepared for each set of wells with 300  $\mu$ L of unsupplemented Sf900 III medium and their varying concentrations of bacmid as well as 6  $\mu$ L of Cellfectin (Invitrogen). 200  $\mu$ L of the corresponding bacmid solutions were added to each well dropwise. The plate was incubated for 5 hours at room temperature, followed by a media change with Sf900 III medium (Thermo scientific) containing 10  $\mu$ g/mL gentamicin (Sigma-Aldrich), 0.01% poloxamer-81 (Sigma-Aldrich), and 1x lipids (Sigma-Aldrich). The plate was then incubated at 27°C and assessed every day after to determine if the cells were transfected. Once the cells reached late stage infection, the cells were scraped off the bottom of the wells and the duplicate wells were pooled. The cell samples were centrifuged at 500 x g for 5 minutes. The supernatant containing the virus was transferred to a dark conical and stored at 4°C until subsequent steps.

#### **2.1.5 Second Amplification of Baculovirus**

To increase the viral titer, a second amplification was needed. 25 mL of Sf9 cells at a concentration of  $1 \times 10^6$  cells/ mL were added to a 75 cm<sup>2</sup> tissue culture flask and were allowed to adhere for 1 hour. 200  $\mu$ L of the first amplification baculovirus were

added to the flask and incubated at 27°C until they reached late stage infection. The cells were collected and centrifuged at 500 x g and 4°C for 5 minutes. The supernatant was collected in a dark 15 mL conical, as with the first amplification virus, and then stored at 4°C.

### **2.1.6 Third Amplification of Baculovirus and Test Expression**

A third amplification was performed to further increase the viral titer and a test expression was performed to determine the resulting potency of the virus. 40 mL of Sf9 cells at a concentration of  $1 \times 10^6$  cells/ mL and 2.5 mL of second amplification virus were added to a 125 mL baffled flask. They were incubated at 27°C and 80 rpm until they were in late stage infection. The cells were then harvested, centrifuged at 500 x g for 5 minutes and the supernatant was transferred to a dark conical and stored at 4°C. To test the potency of the resulting baculoviral a test expression was performed with varying concentrations of virus and the resulting samples were subjected to a western blot to determine the titer and optimal infection conditions.

### **2.1.7 Expression and Purification of PKG I $\alpha$**

Once the viral titer was determined, a full expression of PKG I $\alpha$  and subsequent purification were performed. To a 2.8 L baffled flask, 1 L of Sf9 cells was added at the concentration of  $1.5 \times 10^6$  cells/mL in Sf 900 III media (Thermo scientific). Baculovirus was then added from the third amplification at a volume of  $(1/500) \times$  volume of cells. The cells were incubated at 27°C and 80 rpm for three days. The cells were then harvested, centrifuged at 500 x g for 30 minutes and the supernatant was discarded. 1 mL of a 10x protease inhibitor cocktail was added to the pellet to inhibit proteolysis of PKG. 20 mL of cold lysis buffer (10 mM TES Ph 7, 300 mM NaCl, 5mM imidazole) were added to re-suspend the pellet, and the cells were lysed. The lysate was then centrifuged at 25-40K x g (15K RPM Sorvall SS-34 rotor) for 90 minutes at 4°C. While the lysate was centrifuged, a nickel affinity chromatography column was regenerated with the rational of (**Table 2.2**). The lysate was loaded onto the column and the flow through was collected for each of the subsequent steps. The first wash was performed by running 7 column volumes (CV) of lysis buffer through the column. A second wash was then performed with 5 CV of mid wash buffer (10 mM TES Ph 7, 300 mM NaCl, 3mM imidazole). Once washed, an elution was performed by running the elution buffer (5 mM TES Ph 7, 300mM NaCl, and 250 mM imidazole) through the column; five 5 mL fractions were collected. Qualitative analysis via Bradford assay was performed by combining 20  $\mu$ L of each fraction with 1 mL of 1x Bradford reagent and the color was noted; blue indicated the presence of protein. Once the fractions containing the protein were identified, they were pooled. The pooled fractions were dialyzed in 2 L of dialysis buffer twice (50 mM MES Ph 6.9, 300 mM NaCl, and 1mM Tcep) at 4°C overnight on a stir plate to exchange the buffer. A third dialysis was performed to exchange the buffer to the final storage buffer (50 mM MES ph 6.9, 150 mM NaCl, 1 mM TCEP, and 10% glycerol). The resulting protein concentration

was determined via Nanodrop® spectrophotometry (Fischer scientific) at  $\lambda=280$  nm with the molar coefficient of 81,250, determined by the ProtParam tool (ExPASy).

Solution	Volume (CV)	Concentration
EDTA	10	50 mM
ddH <sub>2</sub> O	2	
NaCl	1	1 M
ddH <sub>2</sub> O	2	
NaOH	1	1 M
ddH <sub>2</sub> O	10	
NiSO <sub>4</sub>	4	1 M
Equilibration Buffer	5	50 mM NaOAc, 300 mM NaCl
ddH <sub>2</sub> O	10	
Lysis buffer	5	10 mM TES Ph 7, 300 mM NaCl, 5mM imidazole
Cell lysate		
Wash buffer 1	7	10 mM TES Ph 7, 300 mM NaCl, 3mM imidazole
Wash buffer 2	5	10 mM TES Ph 7, 300 mM NaCl, 3mM imidazole
Elution buffer	6	(5 mM TES Ph 7, 300mM NaCl, and 250 mM imidazole

**Table 2.2. Nickle affinity chromatography regeneration and purification**

The sequence of events when regenerating the nickel chromatography column and purification of cellular lysate. The regeneration consists of the first 10 steps and the purification is the remaining 4 steps. At the elution, six 5mL fractions are collected.

## 2.2 Peptide Synthesis

The synthetic peptides (S-tides) were synthesized via solid-phase synthesis on Rapp S RAM resin (Rapp Polymere) with a Syro multiple peptides synthesizer (MultiSynTech) by Werner Tegge (Helmholtz Center for Infectious Research). Fmoc solid-phase synthesis was employed with tenfold excess of 2-(1H-Benzotriazole-1-yl)-1,1,3,3-tetramethylaminium tetrafluoroborate (TBTU) and diisopropylethyl amine activation. The coupling reaction was performed for 1 hour. The amino acid sidechains were protected with the following rational: Asp, Glu, Ser, Thr and Tyr: with a tert-butyl group; Asn, Cys, Gln, and His: with a Trityl group; Arg with a 2,2,4,6,7-Pentamethyldihydrobenzofuran-5-sulfonyl (Pbf) group; lys and Trp: with a *tert*-Butyloxycarbonyl group. The resulting peptides were cleaved off the Rapp S RAM resin and the protecting groups were removed with a solution of Trifluoroacetic acid (TFA), 3% triisopropylsilane and 2% water. The peptides were purified via high-performance liquid chromatography (HPLC) and then lyophilized to removing any remaining water.

## 2.3 Circular Dichroism Spectroscopy

To determine the secondary structure of the S1.5 and S2.5 peptides, we employed circular dichroism spectroscopy with the help of Werner Tegge (Helmholtz Center for Infectious Research). The circular dichroism (CD) spectra of S1.5 and S2.5 were measured with a JASCO J-815 circular dichroism spectrometer at 20°C with a cell thickness of 0.5 mm. Each sample measured contained 100 µM peptide in 50 mM sodium phosphate pH 7.0. The samples were scanned at 50 nm / min with a range of 190-300 nm. for each wavelength. 10 replicate scans were performed which were averaged for the resulting spectra of each peptide.

## 2.4 P81 Phosphotransfer-Assay

To test the kinase activity of the purified PKG and the various experimental conditions, a radioactive assay was adapted from the work of (Landgraf and Hofmann., 1989) as well as (Dostmann et al., 1999). In this assay PKG performs a phosphotransferase reaction which transfers the terminal phosphate of a  $P^{32}$  tagged ATP molecule to the basic W15 peptide substrate that has the amino acid sequence TQAKRKKSLAMA (Dostmann et al., 1999). The reaction is transferred to a Whatman P81 phosphocellulose filter paper which binds the substrate and allows for accurate measurement of CPM in a liquid scintillation counter. Based on the degree of radioactivity, the velocity at which the kinase phosphorylates the substrate can be determined. Using a series of increasing concentrations of activator in each reaction we are able to plot the resulting velocities and determine the kinetic profile of different conditions and activators with respect to PKG.

To prepare for the kinase assay, the reactions were labeled and organized in duplicate 1.5 mL Eppendorf tubes with blank, zero and the varying concentrations of cGMP. 10  $\mu$ L of each 10x cGMP stock was aliquoted into their respective tubes and  $DDH_2O$  in the blank and zero. The reaction tubes were stored at 4°C until it was time to run the reaction. The Whatman P81 phosphocellulose filters (2cm/1.9cm) were labeled to their corresponding reaction number. For each reaction, 20  $\mu$ L of 5xMES mix (250 mM MES pH 6.9, 5mM MgOAC, and 50mM NaCl), 10  $\mu$ L of 100 mM DTT, 10  $\mu$ L of 10 mg/mL BSA (Cohn's fraction V), 10  $\mu$ L of 100  $\mu$ M W15 substrate, and 10  $\mu$ L of  $DDH_2O$  were added to a 15 mL conical on ice constituting the batch reaction mix. Prior to adding the ATP to the reaction mix, it had to be spiked with  $P^{32}$  tagged ATP.

To determine the specific activity of the  $P^{32}$  tagged ATP, 10  $\mu\text{L}$  of 1mM for each reaction plus 50  $\mu\text{L}$  was added to an separate tube then  $P_{32}$  tagged ATP was added with the rational that  $1/100 * \text{total volume (ATP)} = \text{volume } P_{32} \text{ ATP added on the 1}^{\text{st}} \text{ day of receiving it and } 1/50^{\text{th}}$  at 1 half-life (14 days). Once the ATP was spiked 5  $\mu\text{L}$  was diluted 1:10 and then in duplicate 10  $\mu\text{L}$  was blotted onto P81 filter papers and then measured in the liquid scintillation counter. Once the specific activity of the ATP was determined, 10  $\mu\text{L}$  for each reaction was added to the reaction mix. 70  $\mu\text{L}$  of the reaction mix was added to each reaction tube. The reactions are activated with the addition of 20  $\mu\text{L}$  of diluted PKG.

A dilution of the PKG stock was created in Enzyme Dilution Buffer (EDB) (50mM MES ph 6.9, 1 mg/mL BSA (cohn's fraction V), 1 mM TCEP, and 50 mM NaCl) resulting in a 10x stock of PKG that corresponds to 8 ng of PKG per reaction ensuring steady state conditions. The reactions were initiated with 20  $\mu\text{L}$  of the diluted PKG (pipetted 10 times for consistency), and 20  $\mu\text{L}$  of ddH<sub>2</sub>O for the blank condition, resulting in a total reaction volume of 100  $\mu\text{L}$ . The reactions proceeded at 30°C for 3 minutes. To terminate the reaction, 50  $\mu\text{L}$  of the reaction was blotted onto its corresponding Whatmann P81 filter paper, which was then washed in 20 nM phosphoric acid 4 times to stop non-specific binding and remove unbound  $P^{32}$ . The filters were dried, placed in scinti vials containing PPO and POPOP in toluene, and their CPM was measured via liquid scintillation counter (Perkin Elmer).

#### **2.4.1 S1.5 and cGMP Pre-Incubation and S-tide Analog Kinetic Assays**

The work of Thomas Moon et al., 2015, established that the binding kinetics for S1.5 was quite slow and that it required pre-incubation with PKG I $\alpha$  in order to activate

it. For this reason, it was necessary to adapt the procedure from section **2.4.0** to allow for a 30 minute incubation prior to activation. The cGMP and S1.5 kinase assays without incubation were conducted with the previously stated procedure using the same set of reagents and timing. The cGMP and S1.5 assays with incubation were performed with the same reagents and concentrations but differed in the setup and initiation. To allow for a 30 minute incubation of PKG with either S1.5 or cGMP, the 10  $\mu$ L of the activator and 20  $\mu$ L of the diluted PKG were added to the reaction tube first and incubated at 30°C for 30 minutes. The reactions were initiated with the addition of 70  $\mu$ L of the reaction mix. The reactions proceeded for 3 minutes and were terminated as previously stated. This method of assay was used to perform the assays in which we tested the new S-tide analogs.

#### **2.4.2 Activator Combination Assays and PKG I $\alpha$ Mutant Assays**

To test the effect of activating PKG I $\alpha$  with a combination of S1.5 and cGMP, the procedure specified in section 1.4.1 was altered slightly allowing for pre-incubation and the addition of another reagent. Like 1.4.1, the activator was combined with the PKG I $\alpha$  for a pre-incubation. In this case it contained 20  $\mu$ L of the PKG dilution, 10  $\mu$ L of the cGMP stock and 10  $\mu$ L of the S1.5 stock. To compensate for the 10  $\mu$ L of the second activator, the 10  $\mu$ L of DDH<sub>2</sub>O was omitted from the reaction mix. After the 30 minute incubation, the reactions were initiated with 60  $\mu$ L of reaction mix. The reactions proceeded for 3 minutes and were terminated in the same manner previously described. To test if S1.5 shares the same degradation of activity as cGMP when activating the C42S mutant, two procedures were used. To establish the kinetics of cGMP on C42S, we employed the same procedure as **2.4.1**. A pre-incubation was needed to activate C42S

with S1.5 due to its slow binding kinetics. The E292A mutant was tested in the same manner as C42S with the addition of a combination assay, as stated previously, to determine the effect of the B-site knockout.

### **2.5.0 Synthesis of P81 Phosphocellulose**

Our protein kinase assay relies on the use of phosphocellulose paper (P81) as a means to trap the enzyme's reaction product, phosphorylated substrate peptide (Dostmann., 2000). When the maker of P81 discontinued its product line, it became vital to develop a protocol for the reliable and sustainable synthesis of phosphocellulose. By utilizing sodium trimetaphosphate ( $P_{3m}$ ) (**Figure 2.5.1**) we succeeded to develop a semi-automatic method by converting 10 x 10cm sheets of regular cellulose filter paper (Whatmann) at PH 12.0 and 50°C (Inoue., 1995).  $P_{3m}$  reacts with hydroxyl-groups of  $\alpha$ -D-glucose and other sugars by a nucleophilic substitution reaction to form mostly monophosphate derivatives. Triphosphate derivatives will also be formed to a lesser degree. The reaction solution was constantly adjusted to PH 12 by addition of 6M NaOH solution. To assure equal reaction conditions for all paper sheets, a device was designed that would hold each sheet in quasi suspension (**Figure 2.5.2**). The device was 3D printed in the lab using ABS (Acrylonitrile butadiene styrene) plastic on a PRUSA I3 MK3 printer. A Büchner funnel holding 6M NaOH and a PH electrode allowed for constant monitoring and addition of NaOH. After a 2 week reaction time, the phosphocellulose sheets were extensively washed, dried in acetone and subsequently in air, and cut to size (2x2 cm). A quality test revealed that our P81-paper had similar capacity and signal stability across all sheets. For this a PKG kinase assay was used under fully saturated conditions.

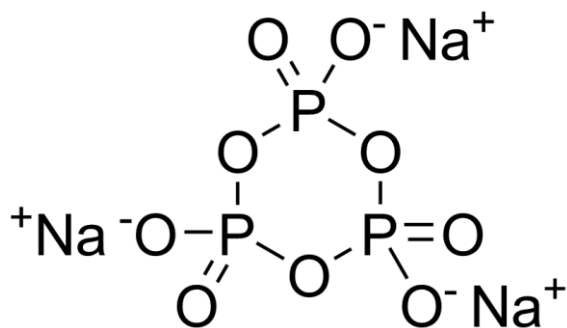


**Figure 2.5.1 Structure of Sodium Trimetaphosphate (P<sub>3m</sub>)**

Above is the structure of the sodium trimetaphosphate (P<sub>3m</sub>) used in the reaction with cellulose paper to result in the synthesis of phosphor cellulose.

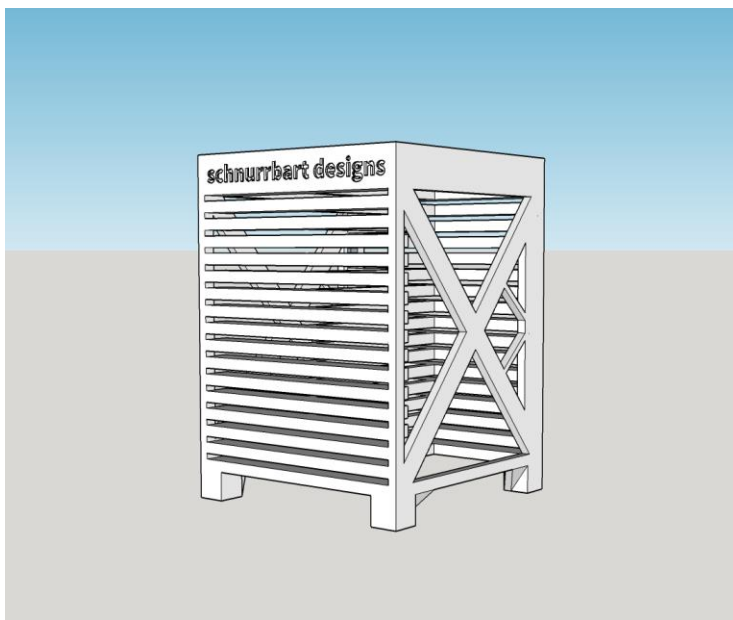


**Figure 2.5.2 P81 Filter Production Device**

The figure above is the final design of the filter suspension system. The holder was designed to fit into a 2 L beaker and produces 16 8x8 filters. The bottom is raised to allow for a stir bar to move freely.

### **2.5.1 Validation of P81 Phosphocellulose**

To determine the efficacy of the phosphocellulose produced in **2.5.0** we employed kinase assays with PKG 1 $\alpha$  as described previously using 5  $\mu$ M cGMP to achieve maximal activation. In order to test the consistency amongst all filter's sheets produced in one synthesis a filter cut from the same location on all sheets were reacted with the same conditions. To test the consistency across the whole filter sheet, the whole sheet was divided into equal 2 x 2 cm and they were reacted with consistent conditions. To overall efficacy of the synthesis the same kinase assay was performed testing our filters against Whatman P81 filters we had saved for this purpose.

### **2.6 Data Analysis**

In order to interpret the data collected from the various experiments conducted in this thesis several programs were employed to covert raw experimental data into usable kinetic information. When the kinase assay is performed we obtain counts per minute (CMP) from the liquid scintillation counter. This data is imported into excel where the average velocity minus the blank is calculated of two replicate counts. The velocity is calculated by multiplying the CMP by the blotting and purity correction and dividing by the reaction time, concentration of protein and the specific activity. This results in the velocity ( $\mu$ mol(P-W15) / min x mg (PKG)). The velocities and their corresponding activator concentrations are then imported into Graphpad Prism<sup>TM</sup> where a nonlinear regression curve fit is performed on velocity vs Log concentration to calculate the kinetic constants  $K_A$ ,  $n_h$ ,  $V_{max}$ ,  $V_{min}$  and fold activation. The non linear curve fit generates the accompanying graphs seen throughout this thesis.

## **3.0 RESULTS**

### **3.1 Protein Expression and Purification**

To explore the objectives of this thesis it was necessary to express and purify recombinant PKG I $\alpha$  wild type as well as the various mutant forms of PKG. The Bac to Bac baculovirus protein expression system (Invitrogen) was employed because bacterial expression of PKG I $\alpha$  has yet to be accomplished (Feil et, Al., 1993). Wild type PKG I $\alpha$  as well as all types of mutant forms of PKG expression and purification has been developed in the Dostmann Lab (Dostmann et,al., 2000; Sheehe., 2018). Likewise the expression the of the mutant forms of PKG I $\alpha$  E292A and C42S was performed using this established protocol.

Following lysis and Ni<sup>2+</sup> affinity chromatography, a correlative Bradford assay was performed on each of the elution samples to determine which fraction contained the protein (**Figure 3.1.1**). To further establish purity of the enzyme preparations, gel electrophoresis using 1mm 4-20% TGX gel, were performed on the clarified lysate (CL), flow through (FL), first wash (W1), second wash (W2), elution 3 (E3), and elution 4 (E4) (**Figure 3.1.2**). From the pooled and dialyzed fractions, the concentrations and total yields were determined (**Figure 3.1.3**). Lastly, to determine if the resulting PKG I $\alpha$  enzymes were pure and functional, a Kinase assay was performed on wild type with varying concentrations from 2 nM – 10  $\mu$ M of cGMP. The resulting data was subjected to a non linear regression curve fit to determine the kinetic characteristic of the enzyme (**Figure 3.1.4**, **Table 3.1.1**). The total yields for the expressions for PKG I $\alpha$  WT, E292A, and C42S were 14.2 mg, 5.4 mg, and 10 mg, respectively. The resulting activity with cGMP was consistent with previously determined data.

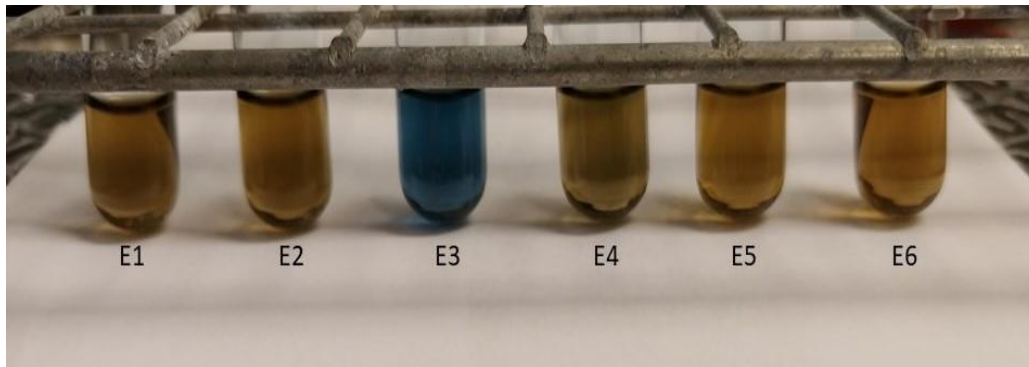


**Figure 3.1.1. Correlative Bradford analysis of PKG I $\alpha$  WT purification Fractions.**

This figure displays the results of combining 5  $\mu$ L of elution fraction to 1 mL of Bradford reagent. The analysis is sequentially elution fractions 1-6. The color change is dependent of the presence of protein from changing from brown to blue when protein is added.

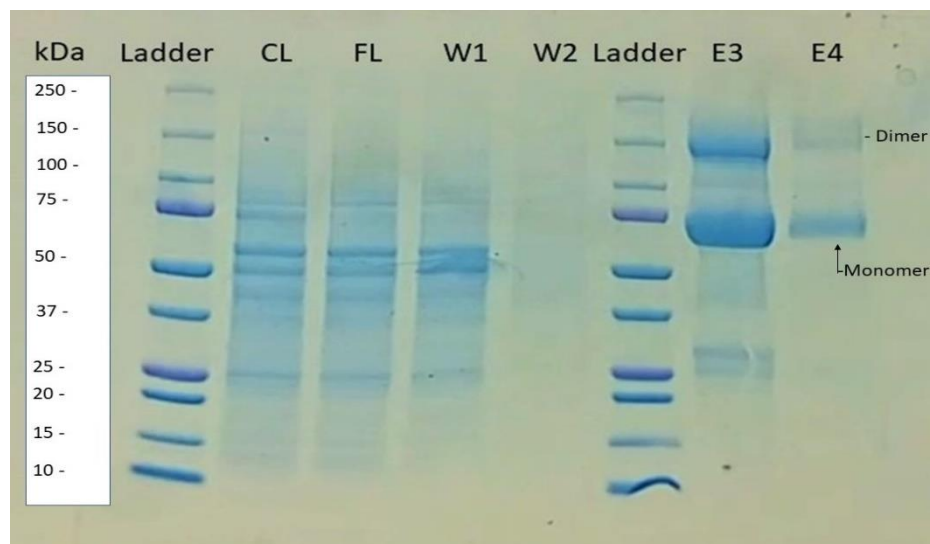


**Figure 3.1.2. Gel electrophoresis of PKG I $\alpha$  WT purification steps.**

The gel above is the result of running 15  $\mu$ L of sample from each step of the Ni affinity chromatography performed on the cellular lysate of *sf9* cells expressing PKG I $\alpha$  WT and 5  $\mu$ L of protein ladder on a 1mm 4-20% TGX protein gel for 30 minutes at 190 V and 0.68A. From left to right the columns were as follows; protein ladder, clarified lysate (CL), flow through (FL), wash 1 (W1), wash 2 (W2), ladder, elution 3 (E3), and elution 4 (E4).

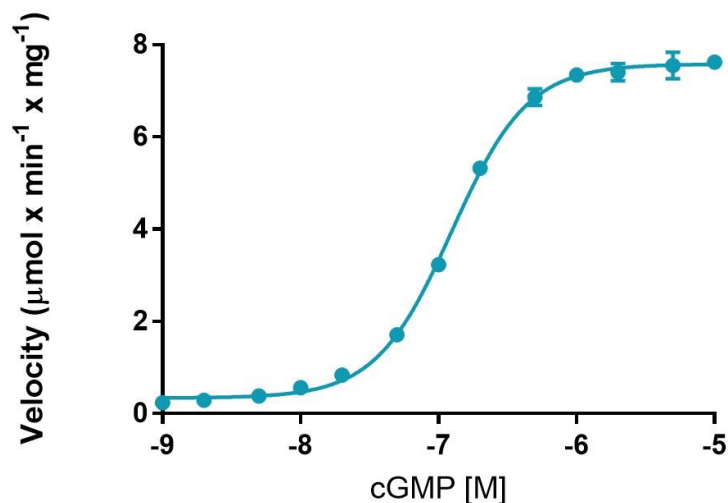


**Figure 3.1.3. Test activation of PKG Iα wild type prep with cGMP.**

Above is a nonlinear regression curve fit of cGMP activated PKG Iα WT (N=2). The curve was created with individual reaction velocity's from 9.3 ng of PKG Iα, varying concentrations of cGMP 2nM – 10 μM and reaction times of 3 minutes. The x-axis displays the log concentration of cGMP and the Y-axis is the reaction velocity in μ mols of phosphorylated w15 substrate per minute mg of PKG Iα.

	<b>cGMP</b>
<b>V<sub>max</sub> (μmol x min<sup>-1</sup> x mg<sup>-1</sup>)</b>	7.6 ± 0.05
<b>V<sub>min</sub> (μmol x min<sup>-1</sup> x mg<sup>-1</sup>)</b>	0.34 ± 0.044
<b>Fold Activation</b>	22.4
<b>n<sub>h</sub></b>	1.58 ± 0.06
<b>K<sub>a</sub> (μM)</b>	0.13 ± 0.064

**Table 3.1.1. Kinetic constants derived from the non linear regression fit of the cGMP PKG Iα activation curve.**

Displayed are the kinetic variables determined from the kinetic analysis in **Figure x**. The experimental conditions are listed in the top row and their corresponding kinetics are in their respective columns. V<sub>max</sub> corresponds the maximal velocity of each curve, n<sub>h</sub> corresponds to the hill coefficient of the curve, and the K<sub>a</sub> is the activation constant of each curve.

### 3.2 Determination of optimal Activation Conditions for S-tide Activation of PKG-I $\alpha$

The work of Moon et al. (2015) explored the idea of synthetic peptides activators of PKG I $\alpha$  derived from the recently discovered switch helix domain and determined the S1.5 peptide (YEDAEAKAYEAEAAFANLKLSD) to be the most active. While studying the peptides binding kinetics it was discovered that it required extended incubation with PKG I $\alpha$  to reach maximal binding. This determines the need for a preincubation of the S-tides with PKG prior to kinetic analysis. This addition to the established P81 phosphoryl transfer assay warranted experimentation to determine the effect that preincubation has on PKG I $\alpha$  wt so that the S1.5 analysis can be deemed valid. It was hypothesized that an incubation of 30 minutes at 30°C would result in ample time for S-tide binding and would not result in any negative effect on the enzyme itself. To test this hypothesis, kinetic assays were performed on PKG-I $\alpha$  WT with both cGMP and S1.5 comparing preincubation and no preincubation. The resulting data by plotting reaction velocity against the Log concentration of activator with a four-parameter nonlinear regression curve fit (Graph pad Prism). Below, the combination graph displaying each condition as well as the table with their respective V<sub>max</sub>, activation constant (K<sub>a</sub>), and hill coefficient (n<sub>h</sub>) (**Figure 3.2.1., Table 3.2.1**). This data shows that there is no effect on the activation profile when the enzyme was activated with cGMP supported by the V<sub>max</sub> of about 4  $\mu\text{mol}(\text{w15-p})/\text{min}\cdot\text{mg}$  and a K<sub>a</sub> of about 100 $\mu\text{M}$  for both trials, which is in agreement with the published values. Conversely preincubation greatly improved the activation of S1.5. As for the S1.5 the no preincubation trial resulted in an activation profile that could not reach maximal velocity at testable concentration, the preincubation S1.5 resulted in hill coefficient (n<sub>h</sub>) of 2.5 and activation constant (K<sub>a</sub>) of about 6  $\mu\text{M}$  which is consistent with previous data (Moon., 2015).

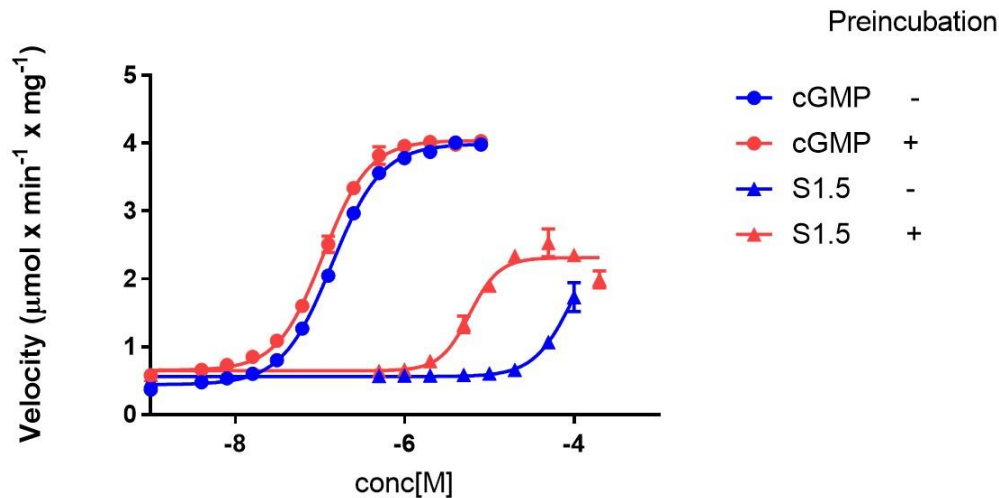


**Figure 3.2.1. Activation curves comparing cGMP V.S. S1.5 and preincubation V.S. no incubation (N=4,2,8,6 respectively).**

The reported Y-axis units are velocity in  $\mu\text{mol}$  of phosphorylated substrate (w15-p) per minute mg of PKG-I $\alpha$  and X-axis units are logarithmic molar concentration of activator (cGMP and S1.5). The increasing concentrations were plotted in order resulting in a sigmoidal curve of PKG-I $\alpha$  activation.

	cGMP Preincubation	cGMP no Preincubation	S1.5 Preincubation	S1.5 no preincubation
$V_{\max}$	$4.04 \pm 0.022$	$4.0 \pm 0.015$	$2.31 \pm 0.034$	-
$V_{\min}$	$0.65 \pm 0.024$	$0.44 \pm 0.014$	$0.65 \pm 0.041$	-
<b>Fold Activation</b>	6.2	9.1	3.6	-
$n_h$	$1.6 \pm 0.06$	$1.5 \pm 0.031$	$2.5 \pm 0.34$	-
$K_a$ [ $\mu\text{M}$ ]	$0.11 \pm 0.06$	$0.14 \pm 0.043$	$5.9 \pm 0.72$	-

**Table 3.2.1. Kinetic constants derived from the activation curves comparing cGMP V.S. S1.5 and preincubation vs no Pre-incubation.**

Displayed are the kinetic variables determined from the kinetic analysis in **Figure 3.2.1**. The experimental conditions are listed in the top row and their corresponding kinetics are in their respective columns.  $V_{\max}$  corresponds the maximal velocity of each curve [ $\mu\text{mol} \times \text{min}^{-1} \times \text{mg}^{-1}$ ],  $n_h$  corresponds to the hill coefficient of the curve, and the  $K_a$  is the activation constant of each curve.

### 3.3 Comparing the Activation Kinetics of S-tide Analogs

Following the discovery that the switch helix can activate PKG-I $\alpha$ , synthetic peptides were created to explore the necessary amino acid residues for optimal activation resulting in the S1.5 peptide (see **section 3.2.**) (Moon et al., 2011, 2015). We worked to further develop the S-tides and target the adjacent cGMP Bite. As part of this study, it was concluded that intermediary peptide was needed to test the removal of the L, S, and D of the S1.5 followed by the addition of a cysteamine linker to increase the binding, the peptides were named S2.5 and S3.5 respectively (**Figure 3.3.1**). The hypothesis was that the removal of the terminal LSD of S1.5 (S2.5) and the addition of the linker (S3.5) would not alter the kinetics of activation of PKG-I $\alpha$ . Kinase assays were performed on S1.5, S2.5 and S3.5 and a nonlinear regression curve fit was performed on the resulting data by plotting the reaction velocity against the logarithm of activator concentration allowing for calculation of the  $V_{max}$ ,  $K_a$ , and  $n_h$  (**Figure 3.3.2., Table 3.3.1**). The results of the S2.5 trials show a significant shift in the activation to the right meaning the activity of the peptide is decreased from what is seen with S1.5. The S3.5 activation was shifted even further, meaning it is even less active and that the addition of the linker further degrades the activity seen in S2.5. when comparing the kinetic constants of all of these S-tides the degradation of activity is seen with the sequential increase in concentration needed to reach the  $K_a$ ; 5.9  $\mu\text{M}$ , 15  $\mu\text{M}$ , and 73  $\mu\text{M}$  for S1.5, S2.5 and S3.5 respectively. A surprising result from this experiment is that the  $V_{max}$  from S1.5: 2.3  $\mu\text{mol(w15-p)}/\text{min}^*\text{mg}$  was severely degraded with the S2.5 modification: 1.6  $\mu\text{mol(w15-p)}/\text{min}^*\text{mg}$ . This degradation of efficacy seems to be fixed by the addition of the linker in S3.5: 2.7  $\mu\text{mol(w15-p)}/\text{min}^*\text{mg}$ , this points to the need of a protecting group at the end of the S-tide. The lack of knowledge of how the holoenzyme is activated warrants further

exploration. We hypothesized that the removal of the C-terminal LSD could cause helical instability and prompted secondary structure analysis of the peptide.

It has been determined that the helicity of the S-tides derived from the switch helix was a crucial factor for activation of PKG I $\alpha$  (Moon et al., 2015). It was concluded that shortening of the S-tides via the C-terminus could disrupt the helicity of the peptide rendering less active. The decrease in activity from S1.5 to S2.5 warranted exploration into the structure of S2.5 and specifically the helical nature of the peptide which has been recognized as a critical part of its function. It was hypothesized that helical instability was the cause of S2.5's impaired activation kinetics. To test this circular dichroism spectroscopy was performed on S2.5. S1.5 was used as a control due to its known helical stability. The secondary structure analysis by circular dichroism spectroscopy results in different characteristic traces based on the secondary structure of the peptide being analyzed, an alpha helix will result in a peak at about 190 nm followed by two consecutive troughs at 205 and 220 nm, a beta sheet will be represented by an initial peak at about 200 nm and a long sloping trough that terminates at 220 nm, as for a random coil the trace would show a trough at 200 nm and peak at 220 nm (Bulheller et al., 2007). The resulting data was graphed, and the two resulting curves were analyzed to determine the difference in helicity. The helical structure of S2.5 is seen to be almost the same as S1.5 (**Figure 3.3.3**), the traces display near identical alpha helix trace characteristics as mentioned earlier, and therefore doesn't explain the shift in activation.

S2.5: Y-E-D-A-E-A-K-A-K-Y-E-A-E-A-A-F-F-A-N-L-K

S3.5: Y-E-D-A-E-A-K-A-K-Y-E-A-E-A-A-F-F-A-N-L-K-G-CH<sub>2</sub>CH<sub>2</sub>-SH

**Figure 3.3.1. Structure of S2.5 and S3.5**

Displayed above are the structures of the S1.5 analogs S2.5 and S3.5 denoted from N to C. The N-terminus of these peptides have an acetyl group conjugated onto it protecting the terminus. The C-terminus of the S2.5 peptide has an amino group attached to protect the terminus.

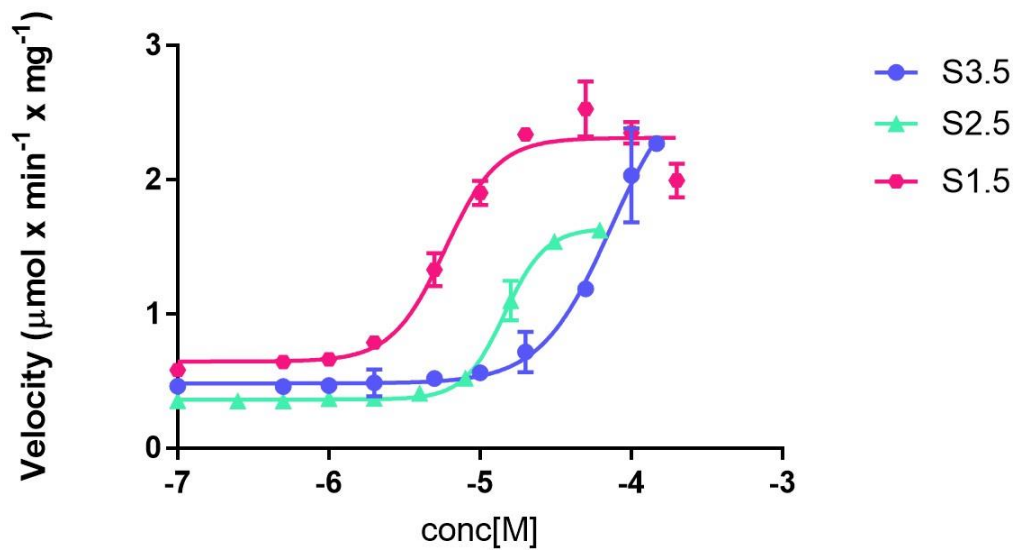


**Figure 3.3.2. Activation Curves Comparing the Kinetics of S1.5, S2.5, and S3.5**

The reported Y-axis units are velocity in μmols of phosphorylated substrate (w15-p) per minute mg of PKG-Iα and X-axis units are logarithmic molar concentration of activator (S1.5, S2.5, and S3.5). The increasing concentrations were plotted in order resulting in a sigmoidal curve of PKG-Iα activation with cGMP control at 5 μM.

	<b>S1.5</b>	<b>S2.5</b>	<b>S3.5</b>
$V_{\max}$ ( $\mu\text{mol} \times \text{min}^{-1} \times \text{mg}^{-1}$ )	$2.31 \pm 0.034$	$1.64 \pm 0.021$	$2.8 \pm 0.25$
$V_{\min}$ ( $\mu\text{mol} \times \text{min}^{-1} \times \text{mg}^{-1}$ )	$0.65 \pm 0.041$	$0.37 \pm 0.01$	$0.49 \pm 0.021$
<b>Fold Activation</b>	3.6	4.5	5.8
$n_h$	$2.5 \pm 0.34$	$3.2 \pm 0.22$	$1.9 \pm 0.26$
$K_a$ [ $\mu\text{M}$ ]	$5.9 \pm 0.73$	$14.5 \pm 0.07$	$73.1 \pm 2.8$

**Table 3.3.1. Kinetic constants derived from activation curves comparing S1.5, S2.5, and S3.5 activation of PKG Ia.**

Displayed are the kinetic variables determined from the kinetic analysis in **Figure 3.3.2**. The experimental conditions are listed in the top row and their corresponding kinetic variables are in their respective columns.  $V_{\max}$  corresponds the maximal velocity of each curve,  $n_h$  corresponds to the hill coefficient of the curve, and the  $K_a$  is the activation constant of each curve.

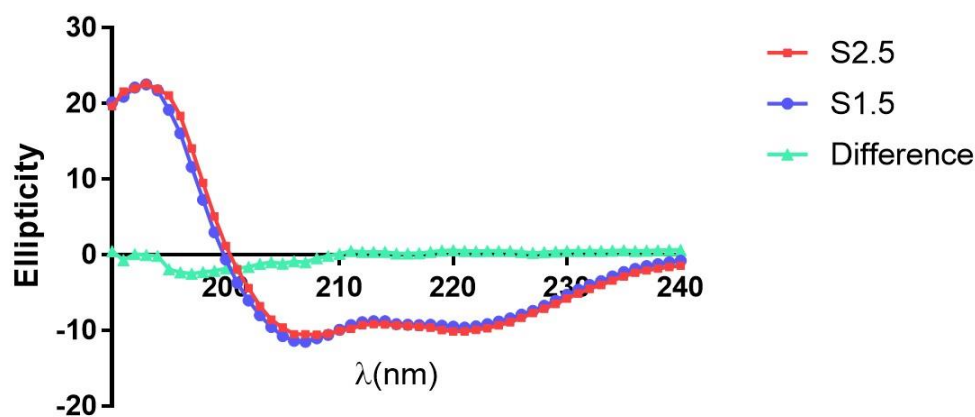


**Figure 3.3.3. Circular Dichroism Helical Profile of S1.5 and S2.5**

The graph plots mean residue ellipticity ( $\theta$ ) mdeg (y-axis) vs the measured wavelength ( $\lambda$ ) in nm (x-axis). The data points are plotted with increasing measured  $\lambda$ . The difference line denoted by the triangular points represent the difference between the S1.5 and S2.5 data points.

### 3.4 PKG I $\alpha$ Co-Activation and Activation Site Interplay.

Our original hypothesis on the mode of activation of S-tides and cGMP proposed a linkage since the SW nest shares residues with the cGMP B-site. However, our findings from the PKG I $\alpha$  C42A trials suggest this may not be the case and prompted further exploration. To further explore the potential interplay between the S1.5 and cGMP binding sites we studied the kinetics of co-activation between the two. We hypothesized that co activation would result in a synergistic activation of PKG I $\alpha$ , if the sites of activation are linked. To test this hypothesis a series of experiments were devised with the rational of performing kinetic assays of cGMP and S1.5 but with the addition of half maximal velocity levels of the other activator. The cGMP assays were performed with varying cGMP concentrations and a constant concentration of S1.5 at 1  $\mu$ M. The S1.5 assays were performed with varying S1.5 concentrations and a constant concentration of cGMP of 100 nM. The resulting data was analyzed by plotting the velocity vs log agonist concentration with a nonlinear regression curve fit to determine the activation kinetics (**Figure 3.4.1. Table 3.4.1.**) The resulting graph shows that the cGMP + 1  $\mu$ M S1.5 had little effect on the overall kinetic profile compared to cGMP alone with a slight shift in the  $K_a$  from about 100 nM to about 140 nM. The addition of 100 nM cGMP to S1.5 resulted in extremely high basal activity of about 50% activation which is expected when using half maximal cGMP. We also saw a shift of  $K_a$  from about 5  $\mu$ M to about 12  $\mu$ M. This decrease in potency is contrary to the idea of synergism but when comparing the  $V_{max}$  of this trial to S1.5 alone we see that the combination assay resulted in 80% maximal activation whereas normally we would only see about 60% activation. This points to the combination causing a decrease in potency but an increase in efficacy. A potential cause of the decrease in potency could be that the cGMP B-site may not be a

site of activation but rather a site of regulation for the SW nest site. This idea prompted us to use more mutant models to explore this possibility even further.

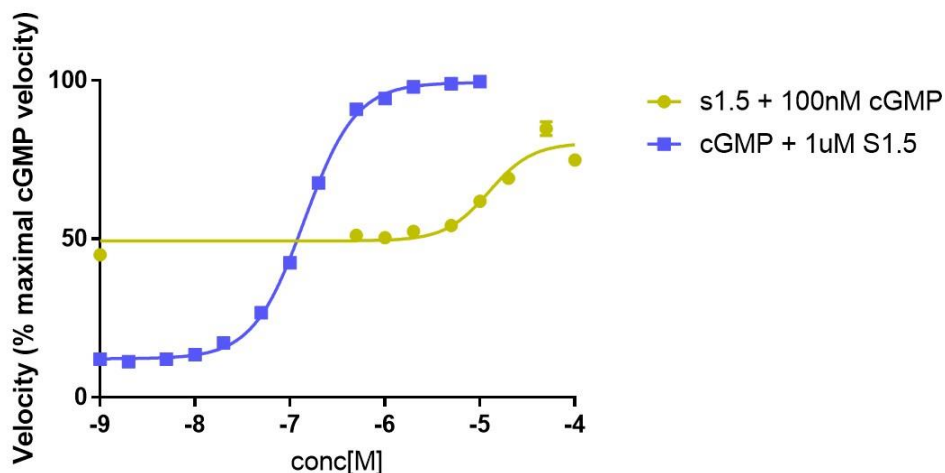


**Figure 3.4.1. Co-Activation curves of cGMP + S1.5 and S1.5 + cGMP. [N=4]**

The reported Y-axis units are normalized percentage of maximal velocity of  $\mu\text{mol}$  of phosphorylated substrate (w15-p) per minute mg of PKG-I $\alpha$ . The S1.5 + cGMP was calculated from a  $5 \mu\text{M}$  cGMP control run at the end of the data set. The X-axis units are logarithmic molar concentration of activator (cGMP and S1.5). The cGMP curve, denoted by the circular data points, had a constant concentration of S1.5 of  $1 \mu\text{M}$  in every reaction. The S1.5 curve, denoted by the triangular data points, had a constant concentration of cGMP of  $100 \text{ nM}$  in every reaction. These curves detail the coactivation of PKG I $\alpha$ .

	<b>cGMP + <math>1 \mu\text{M}</math> S1.5</b>	<b>S1.5 + <math>100 \text{ nM}</math> cGMP</b>
<b><math>V_{\text{max}}</math> (<math>\mu\text{mol} \times \text{min}^{-1} \times \text{mg}^{-1}</math>)</b>	100% $\pm$ 0.33	80.38% $\pm$ 1.97
<b><math>V_{\text{min}}</math> (<math>\mu\text{mol} \times \text{min}^{-1} \times \text{mg}^{-1}</math>)</b>	12.2% $\pm$ 0.29	49.4% $\pm$ 1.05
<b>Fold Activation</b>	8.2	1.63
<b><math>n_{\text{h}}</math></b>	1.61 $\pm$ 0.034	1.9 $\pm$ 0.45
<b><math>K_{\text{a}}</math> [<math>\mu\text{M}</math>]</b>	0.14e-7 $\pm$ 0.04	12.4 $\pm$ 0.34

**Table 3.4.1. Kinetic constants derived from the activation curves comparing co-activation of PKG I $\alpha$  with S1.5 and cGMP.**

Displayed are the kinetic variables determined from the kinetic analysis in **Figure 3.6.1**. The experimental conditions are listed in the top row and their corresponding kinetics are in their respective columns.  $V_{\text{max}}$  corresponds the percentage of maximal cGMP velocity of each curve,  $n_{\text{h}}$  corresponds to the hill coefficient of the curve, and the  $K_{\text{a}}$  is the association constant of substrate binding for each curve.

### 3.5 Activation of PKG I $\alpha$ E292A mutant with cGMP and S1.5

To elucidate the interaction between S-tide and cGMP activation it was determined a mutant protein model where the cGMP B-site was knocked out would give valuable insight into the effect cGMP binding to the B-site has on the activity of S-tides. The rationale for this is that it has been theorized that due to the proximity of the B-site and the switch helix binding site there is site activation interplay. We wanted to test first the effect the E292A mutant would have on normal activation via cGMP and S1.5 when compared to PKG I $\alpha$  WT. Therefore, we performed kinase assays where E292A was activated with cGMP and S1.5. Secondly, we wanted to see what the direct interplay would be if we co-activated the E292A mutant. This experiment is in response to the results of the experiments where we coactivated PKG I $\alpha$  WT, it was thought there would have been synergism but what we saw was the opposite. This led us to the idea that cGMP binding to the B-site might be interfering with the switch helix binding site. To test this, we employed the E292A mutant in a co-activation assay to see if the effect is rectified by the knockout of the B-site. The assays were conducted with constant concentration of one of the activators at half maximal concentration and then a full activation curve of the other activator.

The resulting data was graphed and was subjected to a nonlinear regression curve fit to determine each condition's kinetics (**Figure 3.5.1., Table 3.5.1**). When comparing the kinetics of the cGMP and S1.5 activation of E292A with that of PKG I $\alpha$  WT (**Table 3.5.1**) it is seen that there is no significant change in the kinetic constants. The combination assay where there was 1  $\mu$ M S1.5 and varying concentration of cGMP the resulting activation curve has a slight decrease in  $V_{max}$ ; from 3.021 to 2.56 ( $\mu$ M(W-15 and hill slope potentially). The combination assay in which we had a constant 100 nM cGMP and varying S1.5 concentration we saw a very high basal activity of about half

maximal which is consistent to the wild type combination experiments. This experiment also resulted in a shifted activation in which the  $V_{max}$  was not able to be reached at the concentrations we tested and therefore a significant  $K_a$  could not be calculated but seems to be around 100  $\mu\text{M}$ . This also points to a higher  $V_{max}$  as well pointing to an increase in activity when compared to S1.5 activating E292A by itself which is consistent to the wild type combination assays.

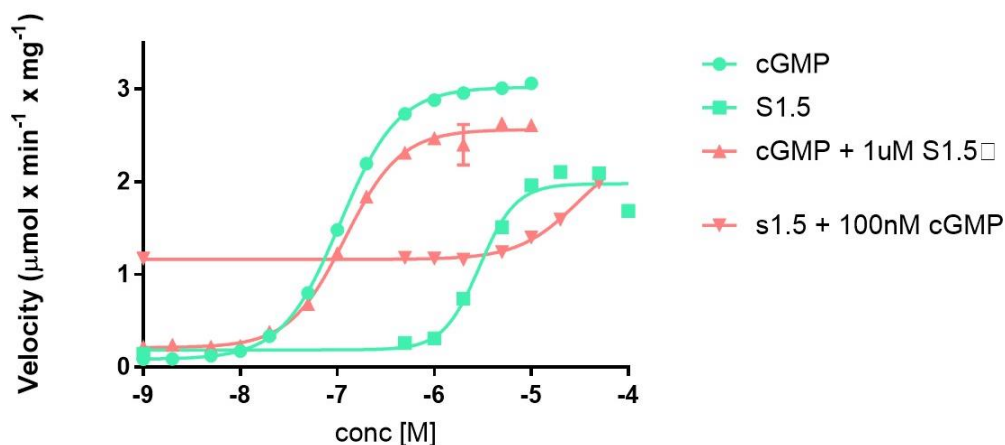


**Figure 3.5.1. Co-Activation of PKG Iα E292A with cGMP [N=4], S1.5 [N=4], cGMP + S1.5 [N=2] and S1.5 + cGMP [N=2]**

The reported Y-axis units are velocity in  $\mu\text{mol}$  of phosphorylated substrate (w15-p) per minute mg of PKG-I $\alpha$  and X-axis units are logarithmic molar concentration of activator (S1.5 and cGMP). The increasing concentrations were plotted in order resulting in a sigmoidal curve of PKG-I $\alpha$  E292A activation in the presence of cGMP, S1.5, cGMP + 1  $\mu\text{M}$  S1.5, S1.5 + 100 nM cGMP.

	cGMP	S1.5	cGMP + 1 $\mu\text{M}$ S1.5	S1.5 + 100 nM cGMP
$V_{\text{max}}$ ( $\mu\text{mol} \times \text{min}^{-1} \times \text{mg}^{-1}$ )	$3.02 \pm 0.012$	$1.98 \pm 0.06$	$2.56 \pm 0.031$	-
$V_{\text{min}}$ ( $\mu\text{mol} \times \text{min}^{-1} \times \text{mg}^{-1}$ )	$0.08 \pm 0.012$	$0.19 \pm 0.07$	$0.21 \pm 0.03$	-
<b>Fold Activation</b>	35.96	10.63	12.2	
$n_h$	$1.45 \pm 0.03$	$2.31 \pm 0.44$	$1.51 \pm 0.11$	-
$k_a$ [ $\mu\text{M}$ ]	$0.10 \pm 0.04$	$2.93 \pm 0.69$	$0.12 \pm 0.13$	-

**Table 3.5.1. Kinetic constants derived from the activation curves comparing co-activation of PKG Iα E292A with S1.5 and cGMP**

Displayed are the kinetic variables determined from the kinetic analysis in **Figure 3.6.1**. The experimental conditions are listed in the top row and their corresponding kinetics are in their respective columns.  $V_{\text{max}}$  corresponds the percentage of maximal cGMP velocity of each curve,  $n_h$  corresponds to the hill coefficient of the curve, and the  $K_a$  is the association constant of substrate binding for each curve.

### 3.6 Efficacy of S1.5 Activation of the Mutant PKG I $\alpha$ C42S

Due to the proximity of the Switch helix binding site to the cGMP B-site it was hypothesized that the cGMP binding site-B and the S-tide binding site (nest) interact. To explore this potential interaction, we determined that mutant enzyme models would be an effective experimental approach. The C42S mutant form of PKG I $\alpha$  has been determined to have diminished activation kinetics with cGMP, demonstrating that the mutation disrupts the pathway in which cGMP activates the enzyme (Sheehe et.al., 2018). We incubated this enzyme with S1.5 to test its activation kinetics. If the two sites communicate, the activation kinetics for S1.5 with C42S would display the marked shift in  $V_{\max}$  and  $K_a$ . To test this hypothesis a series of kinetic assays were performed comparing the activity of S1.5 and cGMP. Statistical analysis was performed on the resulting data by plotting reaction velocity against the logarithm of activator concentration with a nonlinear regression curve fit to determine the kinetic profile of each type of activation. Shown below are a graph and a table displaying the activation curve and the kinetic variables calculated resulting from the experiments. (**Figure 3.6.1., Table 3.6.1.**) PKG C42S shows a remarkable decline in kinetic activity as previously reported (Sheehe et.al., 2018). Not only the  $K_a$  for cGMP is shifted 3-fold shifted from 140  $\mu\text{M}$  (WT) to 450  $\mu\text{M}$  (C42S), the  $V_{\max}$  is also 2-fold reduced from 4  $\mu\text{mol(W15-p)}/\text{min}\cdot\text{mg(PKG)}$  to 2  $\mu\text{mol(W15-p)}/\text{min}\cdot\text{mg(PKG)}$ . Taken together the overall catalytic activity of C42S is less than 10% compared to WT at half maximal activity and approximately 30-50% of full strength of WT. these findings are in agreement with our previously published values. In contest however, the activation kinetics of S1.5 are indistinguishable between C42S and WT. Apparently S1.5 activates

C42S with the same potency and efficacy from WT. These results indicate that the S1.5 binding site operates independently from the cGMP mediated mechanism of action.

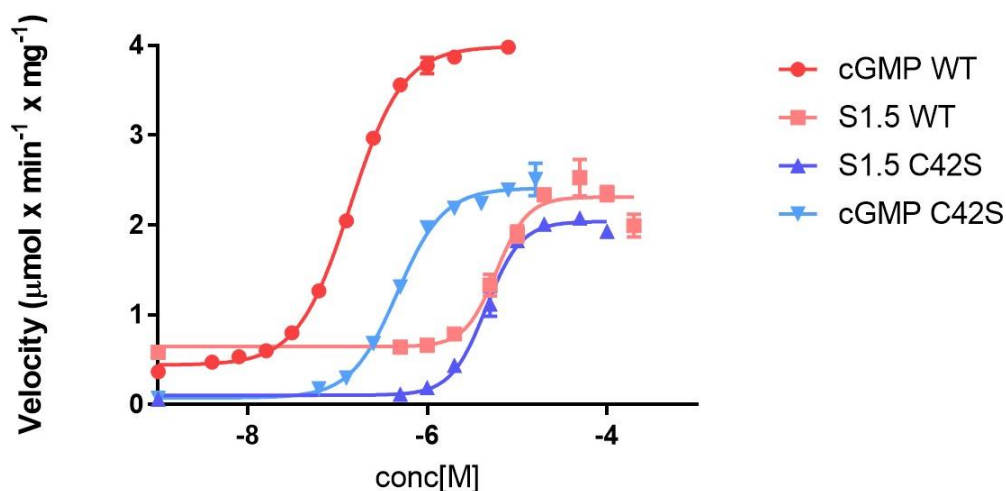


**Figure 3.6.1. Activation curves comparing cGMP (N=2) and S1.5 (N=6) with the PKG Ia C42S mutant V.S. cGMP (N=6) and S1.5 (N=8) activation of PKG Ia WT.**

The reported Y-axis units are velocity in  $\mu\text{mol}$  of phosphorylated substrate (w15-p) per minute mg of PKG-I $\alpha$  and X-axis units are logarithmic molar concentration of activator (S1.5 and cGMP). The increasing concentrations were plotted in order resulting in a sigmoidal curve of PKG-I $\alpha$  C42S mutant and wild type activation. The red curves represent wild type activation and blue represents C42S activation.

	<b>cGMP WT</b>	<b>S1.5 WT</b>	<b>S1.5 C42S</b>	<b>cGMP C42S</b>
<b><math>V_{\max}</math></b> <b>(<math>\mu\text{mol} \times \text{min}^{-1} \times \text{mg}^{-1}</math>)</b>	$4.0 \pm 0.01$	$2.31 \pm 0.03$	$2.04 \pm 0.02$	$2.41 \pm 0.04$
<b><math>V_{\min}</math></b> <b>(<math>\mu\text{mol} \times \text{min}^{-1} \times \text{mg}^{-1}</math>)</b>	$0.44 \pm 0.01$	$0.65 \pm 0.04$	$0.11 \pm 0.02$	$0.08 \pm 0.04$
<b>Fold Activation</b>	9.05	3.29	19.07	31.32
<b><math>n_h</math></b>	$1.48 \pm 0.03$	$2.48 \pm 0.34$	$2.23 \pm 0.13$	$1.67 \pm 0.13$
<b><math>K_a</math> [<math>\mu\text{M}</math>]</b>	$0.14 \pm 0.04$	$5.86 \pm 0.73$	$4.49 \pm 0.29$	$0.46 \pm 0.53$

**Table 3.6.1. Kinetic constants derived from the activation curves comparing cGMP and S1.5 activation of PKG Ia C42S mutant.**

Displayed are the kinetic variables determined from the kinetic analysis in **Figure 3.5.1**. The experimental conditions are listed in the top row and their corresponding kinetic variables are in their respective columns.  $V_{\max}$  corresponds the maximal velocity of each curve,  $n_h$  corresponds to the hill coefficient of the curve, and the  $K_a$  is the activation constant of each curve.

#### **4.0 DISCUSSION AND FUTURE DIRECTIONS**

In this thesis we explored the necessary conditions for the concerted activation of PKG I $\alpha$  using cGMP and peptide analogs derived from the SW domain with the goal to prove or disprove the structure activity relationship between the nucleotide and peptide binding sites. To accomplish these goals, we employed site-specific mutagenesis, secondary structure analysis via circular dichroism spectroscopy, and protein kinase activity assays using the P81 phosphoryl transfer assays. As a result we determined the optimal conditions for kinetic assays, we uncovered the kinetic profile of new PKG I $\alpha$  activators and gained detailed insights into the complex interaction between switch helix and cGMP mediated activation of PKG I $\alpha$ .

The first portion of this thesis was devoted to understanding the requirements of activating PKG I $\alpha$  with S-tides in relationship to cGMP. Through surface plasmon resonance analysis of S-tide association kinetics it was discovered that S-tides require at least 10 minutes to reach peak bound state (Moon et.al., 2015). This discovery warranted an adaptation of the P81 phosphoryl transfer assay where we implemented a 30-minute preincubation at 30 $^{\circ}$ C (reaction temperature) to ensure full binding of the S-tide for each reaction. We compared the cGMP and S1.5 activation with and without the preincubation and determined that the addition of preincubation did not affect cGMP activation but was necessary for S1.5 activation.

After the discovery of the switch helix domain of PKG and S-tide activators the idea of using this as a novel drug target was the logical progression for the Dostmann laboratory. S1.5 is the most potent switch helix analog to date, discovered through careful N and C-terminal truncations, further shortening of the peptide resulted in decreased activity, therefore building upon this peptide was the next step in improving

activity (Moon et.al, 2015). Molecular modeling was employed to determine the structure of a peptide that would interact with the switch helix binding site and the adjacent cGMP B-site. We determined there was a need for intermediary peptides with sequential C-terminus modification. These consisted of S1.5 minus the three C-terminal amino acids (S2.5) and the addition of a cysteamine linker (S3.5) (**Figure 3.3.1**). Both peptides resulted in sequential rightward shifts in  $K_a$  meaning they had decreased activity. This was contrary to the hypothesis. We employed secondary structure analysis of S2.5 and S1.5 to determine if the subtraction of the amino acids was affecting the  $\alpha$ -helicity of the peptides, we determined it was not. Therefore, we cannot explain the decreased activity that easily. These results have caused us to rethink the possible role of the B-site in S-tide activation and caused us to peruse structural analysis of the B-site with regards to S-tide activation to elucidate what is happening. The S3.5 peptide requires further exploration and we have concluded experimentation with S3.5 and mutant forms of PKG I $\alpha$  would serve as way to increase our understanding of the B-site and S-tide activation. We would also like to follow these experiments with surface plasmon resonance assays to determine if S2.5 and S3.5 have different binding and dissociating kinetics than S1.5 which could help explain the shift in the data.

Once we established the need for more exploration of the B-site with respect to S1.5 activation we determined a set of experiments employing activator combination assays and mutant forms of PKG I $\alpha$  would give us valuable insight into the mechanisms at play. To determine the co-dependency between the two mechanisms we performed combination assays where we used both activators to activate PKG I $\alpha$  WT. The results of this experiment showed high basal activity and decrease in potency via a rightward shift in the  $K_a$  when cGMP was added to an S1.5 assay. These results point to some interference between the two pathways of activation. The interference may be caused by

a conformational change of PKG that effects switch helix activity. This led us to believe that the cGMP B-site is potentially acting as a site of regulation for the switch helix binding site and prompted us to use the E292A mutant form of PKG I $\alpha$  which is a B-site knock out to determine the role of the B-site when performing a combination assay. We devised a series of experiments with the E292A mutant first to determine the kinetics of cGMP and S1.5 activation with this mutant followed by activator combination assays. The results of the normal activations established that the E292A mutation does not affect either form of activation compared to PKG I $\alpha$  WT. The combination assay results showed that the cGMP + s1.5 experiment was not affected by the mutation but the S1.5 + cGMP experiment showed an even more significant decrease in potency from the WT combination assay. This is contrary to the hypothesis that the B-site is affecting switch helix binding, if this was the case the  $K_a$  would not have been shifted. This data set only represents an N=2 due to a world-wide shortage of the filter paper that this assay is based off and therefore requires further testing. In the future this assay will be repeated and with higher S1.5 concentrations to reach maximal activity so the kinetic profile could be more accurately evaluated. We would like to follow this up with the E167A mutant which is being produced at the time of this thesis completion. E167A is an A-site knockout which is a dead enzyme, if S1.5 can activate E167A it would support the findings that S1.5 activation is rather cGMP independent.

To help determine if the cGMP and S1.5 activation mechanisms are co-dependent is we used the C42S mutant form of PKG I $\alpha$ , which has a known degradation of cGMP activation when compared to PKG I $\alpha$  WT. We performed kinase assays and determined that the S1.5 activation was normal and was not affected like cGMP. This result shows supports the rejection of the central hypothesis and the idea that S-tide mediated activation is cGMP independent.

This research serves as a platform for future drug development in the critical field of cardiovascular health. PKG is known for its role in smooth muscle relaxation and is the primary effector of the nitric oxide pathway. The nitric oxide pathway has been a major target for antihypertension drugs since the advent of the nitro glycerin therapeutics. PKG would be a prime target for this purpose but due to localization in other areas of the body the problem of off target effects has been the major deterrent. The discovery of the S-tides used in this work serve to be the first isoform specific drug target for PKG I $\alpha$  which would localize the effect of PKG activation to vascular smooth muscle. The further development of these S-tides could usher in a new class of antihypertension agents.

## 5.0 REFERENCES

- Adler, A.J., Greenfield, N.J., Fasman, G.D. (1973). Circular dichroism and optical rotatory dispersion of proteins and polypeptides. *Methods Enzymol* 27, 675.
- Alessi, D.R., Caudwell, F.B., Andjelkovic, M., Hemmings, B.A., and Cohen, P. (1996). Molecular Basis for the Substrate specificity of protein kinase B; comparison with MAPKAP kinase-1 and p70 S6 kinase. *FEBS Lett* 399, 333-338.
- Arencibia, J, Pastor-Flores, D., Bauer A., Schulze, J., Bondi, R. (2013). AGC protein kinases: From structural mechanism of regulation to allosteric drug development for the treatment of human diseases. *Biochimica et Biophysica Acta (BBA) - Proteins and Proteomics*, Vol 1834, Issue 7, 1302-1321.
- Aitken, A., Hemmings, B.A., and Hofmann, F. (1984). Identification of the residues on cyclic GMP-dependent protein kinase that are autophosphorylated in the presence of cyclic AMP and cyclic GMP. *Biochim Biophys Acta* 790, 219-225.
- Atkinson, R.A., Saudek, V., Huggins, J.P., and Pelton, J.T. (1991). <sup>1</sup>H NMR and circular dichroism studies of the N-terminal domain of cyclic GMP dependent protein kinase: a leucine/ isoleucine zipper. *Biochemistry* 30, 9387-9395.
- Bastidas, A.C., Deal, M.S., Steichen, J.M., Guo, Y., Wu, J., and Taylor, S.S. (2013). Phosphoryl transfer by protein kinase a is captured in a crystal lattice. *J Am Chem Soc*, 135(12):4788-98.
- Bolotina, V.M., Najibi, S., Palacino, J.J., Pagano, P.J., and Cohen, R.A. (1994). Nitric oxide directly activates calcium-dependent potassium channels in vascular smooth muscle. *Nature* 368, 850-853.
- Bulheller, B.M., Rodger, A., and Hirst, J.D. (2007). Circular and linear dichroism of proteins. *PCCP* 10.1038/b61587of.
- Casteel, D.E., Zhang, T., Zhuang, S., and Pilz, R.B. (2008). cGMP-dependent protein kinase anchoring by IRAG regulates its nuclear translocation and transcriptional activity. *Cellular signaling* 20, 1392-1399.

D. E. Casteel, E. V. Smith-Nguyen, B. Sankaran, S. H. Roh, R. B. Pilz, and C. Kim. A crystal structure of the cyclic gmp-dependent protein kinase I beta dimerization/docking domain reveals molecular details of isoform-specific anchoring. *J Biol Chem*, 285(43):32684-32688, 2010.

Corbin, J.D., Og Reid, D., Miller, J.P., Suva, R.H., Jastorff, B., and Doskeland, S.O. (1986). Studies of cGMP analog specificity and function of the two intrasubunit binding sites of cGMP-dependent protein kinase. *J Bio Chem* 261, 1208-1214.

Derbyshire, E.R., and Marletta, M.A. (2009). Biochemistry of soluble guanylate cyclase. *Handb Exp Pharmacol*, 17-31.

de Vente, J., Asan, E., Gambaryan, S., Markerink-van Ittersum, M., Axer, H., Gallatz, K., Lohmann, S.S., and Palkovits, M. (2001). Localization of the cGMP-dependent protein kinase type II in rat brain. *Neuroscience* 108, 27-49.

Dey, N.B., Busch, J.L., Francis, S.H., Corbin J.D., and Lincon T.M. Cyclic gmp specifically suppresses type-I-alpha cGMP-dependent protein kinase expression by ubiquitination. *Cell Signal*, 21(6):859-66, 2009.

Orstavik, S., Natarajan, V., Tasken, K., Jahnsen, T., and Sandberg, M. (1997). Characterization of the human gene encoding the type I alpha and type I beta cGMP-dependent protein kinase (PRKG1). *Genomics* 42, 311-318.

Francis, S.H., Smith, J. A., Colbran, J. L., Grimes, K., Walsh, K.A., Kumar, S., and Corbin, J.D. Arginine 75 in the pseudosubstrate sequence of type I beta cGMP-dependent protein kinase is critical for autoinhibition, although autophosphorylated serine 63 is outside this sequence. *J Biol Chem*, 271(34):20748-55, 1996.

Feil, R., Bigl, M., Ruth, P., Hofmann, F. (1993). Expression of cGMP-dependent protein kinase in Escherichia coli. *Mol Cell Biochem*: 127-128:71-80.

Feil, R., Kellermann, J., and Hofmann, F. (1995). Functional cGMP-dependent protein kinase is phosphorylated in its catalytic domain at threonine-516. *Biochemistry* 34, 13152-13158.

Gamm, D.M., Francis, S.H., Angelotti, T.P., Corbin, J.D., and Uhler, M.D. (1995). The type II isoform of cGMP-dependent protein kinase is dimeric and possesses regulatory and catalytic properties distinct from the type I isoforms. *J Biol Chem* 270, 27380-27388.

Heil, W.G., Landgraf, W., Hofmann, F. A catalytically active fragment of cGMP-dependent protein kinase. Occupation of its cGMP-binding sites does not affect its phosphotransferase activity. *Eur J Biochem*, 168(1):117-21, 1987.

Hofmann, F., Dostmann, W., Keilbach, A., Landgraf, W., Ruth, P. (1992). Structure and physiological role of cGMP-dependent protein kinase. *Biochim Biophys Acta*; 1135(1): 51-60.

Hofmann, F., Feil, R., Kleppisch, T., and Schlossmann, J. (2006). Function of cGMP-dependent protein kinases as revealed by gene deletion. *Physiological reviews* 86, 1-23.

Hofmann, F. (2005). The biology of cyclic GMP-dependent protein kinases. *J Biol Chem* 280, 1-4.

Horowitz, A., Menice, C.B., Laporte, R., and Morgan, K.G. (1996). Mechanisms of smooth muscle contraction. *Physiol Rev* 76, 967-1003.

Huang, G.Y., Kim, J.J., Reger, A.S., Lorenz, R., Moon, E.W., Zhao, C., Casteel, D.E., Bertinetti, Vanshouwen, B., Selvaratnam, R., Pflugrath, J.W., Sankaran, B., Melacini, G., Herberg, F.W., and Kim, C. (2014). Structural basis for cyclic-nucleotide selectivity and cGMP-selective activation of PKG I. *Structure*, 22(1):116-24.

Huggins, J.P., Ganzhorn, A.J., Saudek, V., Pelton, J.T., and Atkinson, R.A. (1994). Stimulation of cGMP-dependent protein kinase I alpha by a peptide from its own sequence. An investigation by enzymology, circular dichroism and <sup>1</sup>H NMR of the activity and structure of cGMP-dependent dependent protein kinase I alpha-(546-576)-peptide amide. *European journal of biochemistry / FEBS* 221, 581-593.

Kehrl, J.H., Sinnarajah, S. (2002). RGS2: a multifunctional regulator of G-protein signaling. *Int J Biochem Cell Biol*: 34(5): 432-8.

Kemp, B.E., Cheng, H.C., Walsh, D.A. Peptide inhibitors of camp-dependent protein kinase. *Methods Enzymol*, 159:173-83, 1988.

Kim, C., Cheng, C.Y., Saldanha, S.A., and Taylor, S.S. (2007). PKA-I holoenzyme structure reveals a mechanism for cAMP- dependent activation. *Cell* 130, 1032-1043.

Kim, J.J., Casteel, D.E., Huang, G., Kwon, T.H., Ren, R.K., Zwart, P., Headd, J.J., Brown, N.G., Chow, D.C., Palzkill, T., and Kim, C. (2011). Co-crystal structures of PKG Ibeta (92-227) with cGMP and cAMP reveal the molecular details of cyclic nucleotide binding. *PLoS One* 6, e18413.

Kim, J.J., Lorenz, R., Arold, S.T., Reger, A.S., Sankaran, B., Casteel, D.E., Herberg, F.W., and Kim, C. (2016). Crystal structure of PKG I: cGMP complex reveals a cGMP-mediated dimeric interface that facilitates cGMP-induced activation, *Structure*, 24(5):710-20.

Kuo, I.Y., Ehrlich, B.E. (2015). Signaling in muscle contraction. *Cold Spring Harb Perspect Biol*: 7(2):a006023.

Lalli, M.J., Shimizu, S., Sutliff, R.L., Kranias, E.G., and Paul, R.J. (1999). [Ca<sup>2+</sup>]I homeostasis and cyclic nucleotide relaxation in aorta of phospholamban-deficient mice. *Am J Physiol* 277, H963-970

Landgraf, W., Hofmann, F., Pelton, J.T., Huggins, J.P. Effects of cyclic gmp on the secondary structure of cyclic gmp dependent protein kinase and analysis of the enzyme's amino terminal domain by far-ultraviolet circular dichroism. *Biochemistry*, 29(42):9921-8, 1990.

Manning, G., Whyte, D, B., Martinez, R., Hunter, T., Sadarsanam, S. (2002). The protein kinase complement of the human genome. *Science*: 298(5600): 1912-34.

Morgado, M., Cairrao, E., Santos-Silva, A.J., and Verde, I. (2012). Cyclic nucleotide-dependent relaxation pathways in vascular smooth muscle. *Cellular and molecular life sciences* : CMLS 69, 247-266.

Monken, C.E., and Gill, G.N. (1980). Structural analysis of cGMP-dependent protein kinase using limited proteolysis. *J Bio Chem* 255, 7067-7070.

Moon, T.M., Osborne, B.W., and Dostmann, W.R. (2013). The switch helix: A putative combinatorial relay for inter protomer communication in cGMP-dependent protein kinase. *Biochim Biophys Acta* 1834(7): 1346-1351.

Moon, T.M., Tykocki, N.R., Sheehe, J.L., Osborne, B.W., Tegge, W., Brayden, J.E., and Dostmann, W.R. (2015). Synthetic peptides as cGMP-independent activators of cGMP-dependent protein kinase I $\alpha$ . *Chem Bio*, 22(12): 1653-1661.

Moon, T.M., Sheehe, J.L., Nukareddy, P., Nusch, L.W., Wolfhart, J., Matthews, D.E., Blumenthal, D.K., Dostmann, W.R. (2018). An N-terminally truncated form of cyclic GMP-dependent protein kinase 1 $\alpha$  (PKG I $\alpha$ ) is monomeric and autoinhibited and provides a model for activation.

O'Shea, E.K., Klemm, J.D., Kim, P.S., and Alber, T. (1991). X-ray structure of the GCN4 leucine zipper, a two-stranded, parallel coiled coil. *Science* 254, 539-544.

S. Orstavik, M. Sandberg, D. Berube, V. Natarajan, J. Simard, U. Walter, R. Gagne, V. Hansson, and T. Jahnsen. Localization of the human gene for the type i cyclic gmp-dependent protein kinase to chromosome 10. *Cytogenet Cell Genet*, 59(4):270-3, 1992.

S. Orstavik, V. Natarajan, K. Tasken, T. Jahnsen, and M. Sandberg. Characterization of the human gene encoding the type i alpha and type i beta cgm- dependent protein kinase (prkg1). *Genomics*, 42(2):311-8, 1997.

Osborne, B.W., Wu, J., McFarland, C.J., Nickl, C.K., Sankaran, B., Casteel, D.E., Woods, Jr., Kornev, A.P., Taylor, S.S., Dostmann, W.R. (2011). Crystal structure of cGMP-dependent protein kinase reveals novel site of interchain communication. *Structure*, 19(9):1317-27.

Pearce, L.R., Komander, D., and Alessi, D.R. (2010). The nuts and bolts of the AGC protein kinases. *Nat Rev Mol Cell Biol* 11, 9-22.

Pfeifer, A., Ruth, P., Dostman, W., Sausbeir, M., Klatt, P., Hoffman, F. (1999). Structure and function of cGMP-dependent protein kinases. *Rev Physiol Biochem Pharmacol*: 135: 105-49.

L. Qin, A. S. Reger, E. Guo, M. P. Yang, P. Zwart, D. E. Casteel, and C. Kim. Structures of cGMP-dependent protein kinase (PKG) I $\alpha$  leucine zippers reveal an interchain disulfide bond important for dimer stability. *Biochemistry*, 54(29): 4419-4422, 2015.

P. Ruth, W. Landgraf, A. Keilbach, B. May, C. Egleme, and F. Hofmann. The activation of expressed cGMP-dependent protein kinase isozymes I $\alpha$  and I $\beta$  is determined by the different amino-termini. *Eur J Biochem*, 202(3): 1339-1344, 1991.

Ruth, P., Pfeifer, A., Kamm, S., Klatt, P., Dostmann, W.R., and Hofmann, F. (1997). Identification of the amino acid sequences responsible for the high affinity activation of cGMP kinase I $\alpha$ . *J Bio Chem* 272, 10522-10528.

Schlossmann, J., Desch, M., cGK substrates. *Handb Exp Pharmacol*, (191): 163-93, 2009.

Schnell, J.R., Zhou, G.P., Zweckstetter, M., Rigby, A.C., and Chou, J.J. (2005). Rapid and accurate structure determination of coiled-coil domains using NMR dipolar couplings: application to cGMP-dependent protein kinase I $\alpha$ . *Protein Sci* 14, 24141-2428

Sheehe, J.L., Bonev, A.D., Schmoker, A.M., Ballif, B.A., Nelson, M.T., Moon, T.M., Dostmann, W.R. (2018). Oxidation of cysteine 117 stimulates constitutive activation of type I $\alpha$  cGMP-dependent protein kinase. *J Bio Chem*: 10.1074/lbc.RA118.004363.

Shin, H.M., Je, H.D., Gallant, C., Tao, T.C., Hartshorne, D.J., Ito, M., and Morgan, K.G. (2002). Differential association and localization of myosin phosphatase subunits during agonist-induced signal transduction in smooth muscle. *Circ Res* 90, 546-553.

Sun, X., Kaltenbronn, K.M., Steinberg, T.H., and Blumer, K.J. (2005). RGS2 is a mediator of nitric oxide action on blood pressure and vasoconstrictor signaling. *Mol Pharmacol* 67, 631-639.

Scholten, A., Fuss, H., Heck, A.J., Dostmann, W.R. The hinge region operates as a stability switch in cgmp-dependent protein kinase I alpha. *FEBS J*, 274 (9):2274-86, 2007.

Smith, C.M., Radzio-Andzelm, E., Madhusudan, Akamine, P., and Taylor, S.S. (1999). The catalytic subunit of cAMP-dependent protein kinase: prototype for an extended network of communication. *Prog Biophys Mol Biol* 71, 313-341.

Steichen, J.M., Kuchinskas, M., Keshwani, M.M., Yang, J., Adams, J.A., Taylor, S.S. (2012). Structural basis for the regulation of protein kinase a by activation loop phosphorylation. *J Bio Chem*, 287(18):14672-80.

Takio, T., Smith, S.B., Walsh K.A., Krebs, E.G., and Titani, K., Amino acid sequence around a "hinge" region and its "autophosphorylation" site in bovine lung cgmp-dependent protein kinase. *J Bio Chem*, 258(9): 5531-6, 1983.

Taylor, S.S., Kim, C., Vigil, D., Haste, N.M., Yang, J., Wu, J., and Anand, G.S. (2005). Dynamics of signaling by PKA. *Biochim Biophys Acta* 1754, 25-37.

Wang, G., Jacquet, L., Karamariti, E., Xu, Q. (2015). Origin and differentiation of vascular smooth muscle cells. *J Physiol*: 593(14):3013-30.

Wooldridge, A.A., MacDonald, J.A., Erdodi, F., Ma, C., Borman, M.A., Hartshorne, D.J., and Haystead, T.A. (2004). Smooth muscle phosphatase is regulated in vivo by exclusion of phosphorylation of threonine 696 of MYPT1 by phosphorylation of Serine 695 in response to cyclic nucleotides. *J Biol Chem* 279, 34496-34504.

Wernet, W., Flockerzi, V., and Hofmann, F. (1989). The cDNA of the two isoforms of bovine cGMP-dependent protein kinase. *FEBS letters* 251, 191-196.